ASL-TR-0043

AD A078213

LEVEL

THE ROLE OF ATMOSPHERIC SULFATES IN BATTLEFIELD OBSCURATIONS

D D C
RECEIVED
DEC 14 1979
E

OCTOBER 1979

By

STEPHEN L. COHN

DDC FILE COPY

U.S. ARMY
E RADCOM

US Army Electronics Research and Development Command
ATMOSPHERIC SCIENCES LABORATORY
White Sands Missile Range, NM 88002

79 12 13 052

NOTICES

U.S. MAIL

DEPARTMENT OF THE ARMY
US ARMY ATMOSPHERIC SCIENCES LABORATORY
DELAS-DM-A
WHITE SANDS MISSILE RANGE, NM 88002

OFFICAL BUSINESS
Penalty For Private Use, $300

DEFENSE DOCUMENTATION CENTER
ATTN: DDC-TCA
CAMERON STATION, BLDG 5
ALEXANDRIA, VA 22314
12

ERRATA FOR ASL-TR-0043

THE ROLE OF ATMOSPHERIC SULFATES IN BATTLEFIELD OBSCURATIONS

Page 29   Change second sentence from top of page to read as follows:

$3\mu g/m^3$ were found in the Illinois-Missouri area (figure 8).

REPORT DOCUMENTATION PAGE		READ INSTRUCTIONS BEFORE COMPLETING FORM
1. REPORT NUMBER ASL-TR-0043	2. GOVT ACCESSION NO.	3. RECIPIENT'S CATALOG NUMBER
4. TITLE (and Subtitle) THE ROLE OF ATMOSPHERIC SULFATES IN BATTLEFIELD OBSCURATIONS.		5. TYPE OF REPORT & PERIOD COVERED Technical Report.
		6. PERFORMING ORG. REPORT NUMBER
7. AUTHOR(s) Stephen L. Cohn		8. CONTRACT OR GRANT NUMBER(s)
9. PERFORMING ORGANIZATION NAME AND ADDRESS Atmospheric Sciences Laboratory White Sands Missile Range, NM 88002		10. PROGRAM ELEMENT, PROJECT, TASK AREA & WORK UNIT NUMBERS DA Task 1L162111AH71-26
11. CONTROLLING OFFICE NAME AND ADDRESS US Army Electronics Research and Development Command Adelphi, MD 20783		12. REPORT DATE October 1979
		13. NUMBER OF PAGES 45
14. MONITORING AGENCY NAME & ADDRESS(if different from Controlling Office)		15. SECURITY CLASS. (of this report) UNCLASSIFIED
		15a. DECLASSIFICATION/DOWNGRADING SCHEDULE

16. DISTRIBUTION STATEMENT (of this Report)

Approved for public release; distribution unlimited.

17. DISTRIBUTION STATEMENT (of the abstract entered in Block 20, if different from Report)

ERADCOM/ASL-TR-0043

18. SUPPLEMENTARY NOTES

19. KEY WORDS (Continue on reverse side if necessary and identify by block number)

Battlefield obscuration
Atmospheric sulfates
Atmospheric pollutants

20. ABSTRACT (Continue on reverse side if necessary and identify by block number)

"Seeability" is one of the Army's major concerns in future battle scenarios. With increasing amounts of anthropogenic aerosols present in the atmosphere, seeability in both the visible and near infrared regions of the spectrum is being adversely affected.

Sulfur dioxide, the primary form of anthropogenic atmospheric sulfur, is converted from a gas to a solid (ammonium sulfate) by oxidizing with ammonia gas.

DD FORM 1473 EDITION OF 1 NOV 65 IS OBSOLETE

1

20. ABSTRACT (cont)

Under high humidity conditions (> 80 percent) ammonium sulfate changes from a solid to a liquid with a corresponding four-fold increase in light scattering effectiveness. This report documents the simultaneous occurrence of high concentrations of aerosol sulfur during periods of high humidity and haze. It suggests that ammonium sulfate aids in the formation of haze which affects Army weapon and reconnaissance systems.

PREFACE

The basis of this report originated as a master's degree thesis and was condensed to address current Army problems concerning the electro-optical atmosphere. Although the original investigation of particulate sulfur concentrations was based on data acquired in the Midwestern and Northeastern United States, the results may be equally applicable to the European Scenario due to the similar latitude and climate.

Accession For		
NTIS GRA&I	✓	
DDC TAB	☐	
Unannounced	☐	
Justification		
By		
Distribution/		
Availability Codes		
Dist	Avail and/or special	
A		

CONTENTS

INTRODUCTION

An old maxim concerning combat states that "what can be seen can be annihilated." This concept today is no longer true. Although an observer might detect a target by using an infrared scope, the weapon system that might be employed to engage the target might operate on a different wavelength which is unable to "see" the target. Thus, winning the battle depends on "seeing" and "not being seen," which in turn depends upon factors affecting battlefield obscuration.

There are obvious differences of night versus day and the limitation imposed by terrain and vegetation. These are factors which can be reckoned with because of their stationary character. On the other hand, there are highly variable atmospheric phenomena affecting battlefield obscuration which have the potential to turn the tide of battle one way or another, depending on the circumstances. Some of the more obvious atmospheric phenomena which could affect battlefield obscuration are fog, rain, snow, and dust. One of the less obvious atmospheric elements which has become increasingly important to battlefield obscuration is anthropogenic aerosol, or air pollution as it is more commonly known.

An important problem has been a lack of understanding of the spatial and temporal behavior, as well as the composition of pollutants with identifiable air masses. This problem is due to the lack of suitable large-scale air quality network data.[1] This report addresses the problem in relation to the following meteorological parameters:

1. Visibility degradation (obscuration) with emphasis on haze

2. Relative humidity

These parameters were chosen because earlier studies indicated that ammonium sulfate is the primary sulfate found in the atmosphere. Although windspeed and wind direction, relative humidity, and precipitation all affect the concentration and physical properties of this sulfate, only relative humidity will be discussed in this report. Also, this sulfate is a highly efficient light scattering aerosol that is a likely candidate for visibility obscuration, especially during occurrences of haze. This supposition is supported by past studies where large areas of the Midwestern and Northeastern United States were shown to have typical concentrations of $20\mu g/m^3$ of ammonium

---

[1]R. B. Husar et al., 1976, "Long range transport of pollutants observed through visibility contour maps, weather maps, and trajectory analysis," Third Symposium on Atmospheric Turbulence, Diffusion, and Air Quality, given by the American Meteorological Society on 19-22 October, 1976, Raleigh, NC, 344-347

sulfate during the summer months.[2] Husar et al. measured similar concentrations in Saint Louis during periods of reduced visibility and haze and suggested that sulfates may be one of the primary causes of visibility degradation.[1] In fact, there is an inverse relationship between prevailing visibility and pollutant mass concentration of the form $V \propto \frac{1}{m}$ where m is the mass concentration.[3]

THEORY

The two most common sulfate compounds in the ambient atmosphere are ammonium sulfate $((NH_4)_2SO_4)$ and sulfuric acid (H_2SO_4).[4] Knowledge of which compound is dominant is important in devising future planning strategies. Past studies indicate that sulfates are more effective light scatterers per unit mass than other suspended particulate constituents.[5] Sawyer found that when sulfates are exposed to high humidity, haze is a likely result. He also determined that ammonium sulfate, because of its large light scattering coefficient, is the most effective haze producing aerosol in the Northeastern United States.

Figure 1 shows the results of an experiment[6] where laboratory air was sampled by two cascade impactors. One of the impactors sampled aerosol particles after passing the air through a tube half filled with water so

---

[2]E. Y. Tong et al., 1976, "Regional and local aspects of atmospheric sulfates in the northeast quadrant of the United States," Third Symposium on Atmospheric Turbulence, Diffusion, and Air Quality, given by the American Meteorological Society on 19-22 October 1976, Raleigh, NC, pp 307-310

[1]R. B. Husar et al., 1976, "Long range transport of pollutants observed through visibility contour maps, weather maps, and trajectory analysis," Third Symposium on Atmospheric Turbulence, Diffusion, and Air Quality, given by the American Meteorological Society on 19-22 October 1976, Raleigh, NC, 344-347

[3]S. J. Williamson, 1973, Fundamentals of Air Pollution, Reading, MA, Addison-Wesley Publishing Company

[4]P. R. Ehrlich, Anne H. Ehrlich, and John P. Holdren, 1977, Ecoscience, San Francisco, W. H. Freeman and Company

[5]J. W. Sawyer, 1978, "The sulfur we breathe," Environment, 20:25-26

[6]M. S. Ahlberg, A. C. D. Leslie, and J. W. Winchester, 1978, "The chemical state of particulate sulfur in ambient aerosols determined by PIXE analysis," Nucl Instr and Meth, 149:451-455

as to increase the relative humidity. The other impactor sampled the air directly without humidification. Therefore each experiment consisted of two samples: one humidified sample and one ambient air sample. Near the top of the graph, the humidities of the pairs of samples are indicated. Mass median aerodynamic diameters (MMAD) of particles in each sample were calculated from the measured concentrations in the impactor size fractions, and the MMAD for each humidified sample was expressed relative to the corresponding unhumidified sample MMAD set equal to unity. These values of MMAD were plotted versus the relative humidity at which the samples were taken. The two curves in this graph are the theoretical growth of ammonium sulfate ($(NH_4)_2SO_4$) and sulfuric acid (H_2SO_4) with rising relative humidity. By examining the results of the experiment, one can see that almost all of the points lie on or above the $(NH_4)_2SO_4$ curve, while only a few lie between the curves. Above 81 percent relative humidity, there are no points between the curves. At this relative humidity, $(NH_4)_2SO_4$ undergoes a phase change from solid to aqueous solution with a corresponding increase of a factor of 1.3 in MMAD. The degree of growth of the $(NH_4)_2SO_4$ droplets is greater than for H_2SO_4 for relative humidities up to 95 percent. It is significant that there are no points between the curves above the phase change of $(NH_4)_2SO_4$ and the 95 percent relative humidity point, indicating that a large majority of the sulfur in the laboratory air was ammonium sulfate rather than sulfuric acid.

This experimental result suggests that haze, which frequently forms when relative humidities are between 80 and 95 percent, is due to the rapid growth of $(NH_4)_2SO_4$ after reaching a relative humidity of 81 percent, and therefore ammonium sulfate could be a major contributor to the formation of haze. Once the $(NH_4)_2SO_4$ aerosol is optically activated when it undergoes the transition from solid to aqueous, the reverse process may not take place until relative humidity has decreased to below 30 percent, owing to crystal nucleation reaction kinetics. Therefore, if haze is caused by $(NH_4)_2SO_4$ during periods of high relative humidities, the haze may likely remain even when relative humidities drop well below 80 percent.

Since the primary form of sulfur pollution in the atmosphere is SO_2 (EPA[7]), its properties should be examined. Table 1 shows five possible mechanisms for SO_2 conversion to $SO_4^=$. As indicated in the table, SO_2 changes to $(NH_4)_2SO_4$ if there is enough ammonia present in the atmosphere.

---

[7]US Environmental Protection Agency, 1975, Position paper on regulation of atmospheric sulfates, EPA-450/2-75-007, Research Triangle Park, NC
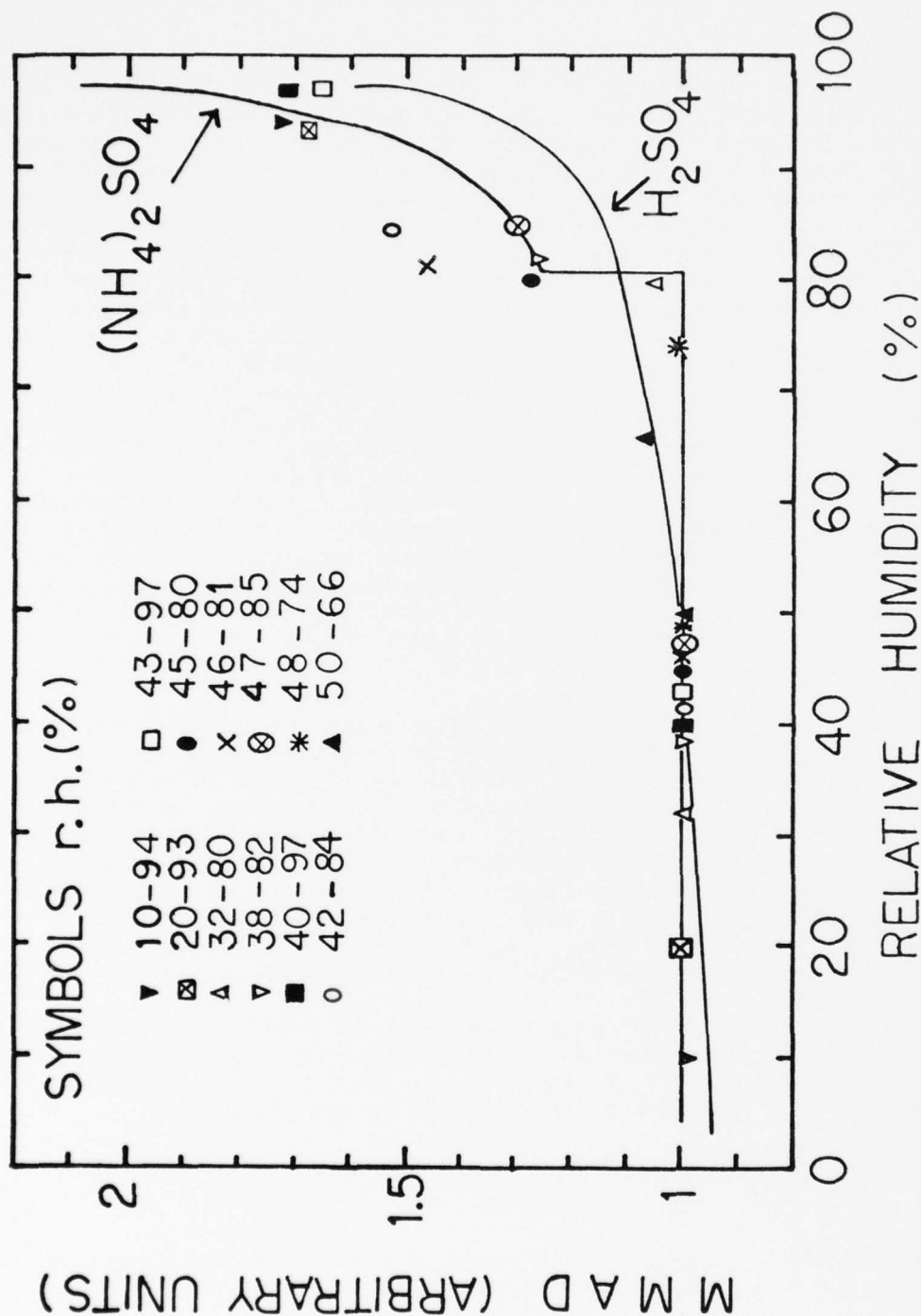
Figure 1. Growth rate of the ambient sulfate aerosol at varying relative humidities as compared to the theoretical growth curves of $(NH_4)_2SO_4$ and H_2SO_4. Each pair of numbers represents the relative humidity of both the ambient and humidified sulfur sample taken at the same time. These results were obtained under controlled conditions by Mats Ahlberg.

TABLE 1. MECHANISMS THAT CONVERT SULFUR DIOXIDE TO SULFATES[7]

Mechanism	Overall Reaction	Factors on Which Sulfate Formation Primarily Depends
Direct photo-oxidation	$SO_2 \xrightarrow[\text{water}]{\text{light, oxygen}} H_2SO_4$	Sulfur dioxide concentration, sunlight intensity.
Indirect photo-oxidation	$SO_2 \xrightarrow[\substack{\text{organic oxidants,} \\ \text{hydroxyl radical (OH)}}]{\text{smog, water, NO}_x} H_2SO_4$	Sulfur dioxide concentration, organic oxidant concentration, OH, NO_x
Air oxidation in liquid droplets	$SO_2 \xrightarrow{\text{liquid water}} H_2SO_3$ $NH_3 + H_2SO_3 \xrightarrow{\text{oxygen}} NH_4 + SO_4^=$	Ammonia concentration
Catalyzed oxidation in liquid droplets	$SO_2 \xrightarrow[\text{heavy metal ions}]{\text{oxygen, liquid water}} SO_4^=$	Concentration of heavy metal (Fe, Mn) ions
Catalyzed oxidation on dry surfaces	$SO_2 \xrightarrow[\text{carbon,water}]{\text{oxygen,particulate}} H_2SO_4$	Carbon particle concentration (surface area)

[7]US Environmental Protection Agency, 1975, Position paper on regulation of atmospheric sulfates, EPA-450/2-75-007, Research Triangle Park, NC
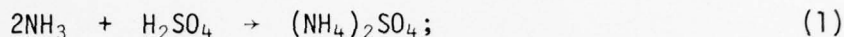
Not shown in the table is that the H_2SO_4 may be neutralized by NH_3 via the following process:

$$2NH_3 \ + \ H_2SO_4 \ \rightarrow \ (NH_4)_2SO_4; \qquad\qquad (1)$$

and, depending on their relative atmospheric abundances, either all the NH_3 or all the H_2SO_4 may be used up.

Over half the land east of the Rocky Mountains is farm land. Nitrogen compounds are important fertilizers used in this area and are a major source of atmospheric ammonia by the process of ammonification.[4] This process frees ammonia by reducing nitrogen compounds in the soil:

$$2NO_2^- \ + \ 4H^+ \ + \ 2H_2O \rightarrow \ 2NH_4^+ \ + \ 3O_2 \ . \qquad\qquad (2)$$
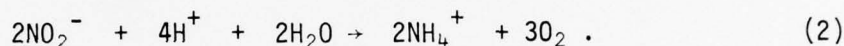
In addition, the decay of vegetable and animal matter releases NH_3 to the atmosphere. It would seem that there are ample sources in agricultural areas for atmospheric ammonia, and $(NH_4)_2SO_4$ should be the most abundant sulfate compound in the atmosphere under these conditions.

If ammonium sulfate is the principal particulate sulfate, we should determine whether this sulfate, in the concentrations encountered by previous studies ($10\text{-}30\mu g/m^3$), can reduce visibility to the levels that are frequently observed during visibility obscuration occurrences by mechanisms other than fog or precipitation.

The extinction coefficient of an aerosol is equal to the sum of its scattering coefficient and its absorption coefficient

$$b_e \ = \ b_s \ + \ b_a \ . \qquad\qquad (3)$$

The scattering coefficient, b_s, is equal to the sum of the molecular scattering, b_{mol}, and the scattering by all the particulates, b_s'.

$$b_s \ = \ b_{mol} \ + \ b_s' \ . \qquad\qquad (4)$$

The term b_{scat} frequently used in the literature refers to b_s of which b_s' may be the larger contributor.

---

[4]P. R. Ehrlich, Anne H. Ehrlich, and John P. Holdren, 1977, Ecoscience, San Francisco, W. H. Freeman and Company

For ammonium sulfate, b_a, the absorption coefficient, is negligible in the visible range;[8] i.e., $b_s >> b_a$. Therefore $b_s \simeq b_e$ and only b_s need be calculated. The type of light scattering that is of interest here is mainly Mie scattering. For the purpose of this model, we assume that the aerosol particles are of a uniform spherical shape and are homogeneous in composition. We also assume relative humidity < 70 percent so that the particles are solid crystals. The scattering coefficient is defined as follows:

$$b_s' = \frac{\pi D_p^2}{4} \int_{\lambda_1}^{\lambda_2} K_s(\lambda, D_p, m) I(\lambda) d\lambda \tag{5}$$

m = refractive index

D_p = diameter of the aerosol particle

K_s = scattering efficiency

$I(\lambda)$ = the normalized intensity distribution of solar radiation at sea level

λ = wavelength

$$I(\lambda) = P(\lambda) / \int_{\lambda_1}^{\lambda_2} P(\lambda) d\lambda \tag{6}$$

$P(\lambda)$ = in watts cm^{-2} m^{-1} = solar spectral irradiance averaged over a small bandwidth centered at λ

$$\int_{\lambda_1}^{\lambda_2} P(\lambda) d\lambda \simeq \sum_1^n P(\lambda_i) \Delta\lambda \tag{7}$$

n = 12

$\Delta\lambda$ = 0.03μm

The scattering coefficient can be estimated by the following equation:

[8]Sheldon K. Friedlander, 1977, Smoke, Dust, and Haze, New York, Wiley

13

$$b_s' \simeq \left(\frac{\pi D_p^2}{4}\right) \left[1/\sum_1^n P(\lambda_i)\right] \sum_1^n K_s(\lambda_i) \, P(\lambda_i) \ . \tag{8}$$

By summing $P(\lambda_i)$, with $\Delta\lambda = 0.03\mu m$ from $0.35\mu m$ to $0.68\mu m$ (visible range), $\Sigma \, P(\lambda_i) = 1.952$.[9]

A realistic calculation of the visibility reducing capabilities of ammonium sulfate should be based on a measured particle size distribution. Figure 2 gives median values for sulfur concentrations in six size ranges at five locations that were sampled by cascade impactors by Winchester in April of 1976. The percentage of sulfur found in each size range is the following:

Impactor Stages	6	5	4	3	2	1
			Percentage			
X New Hampshire	46	31	13	5	3	2
0 St. Louis West	35	46	9	5	3	2
0 St. Louis City	33	40	17	5	3	2
+ Colorado	37	36	22	2	2	1
# New Mexico	22	42	23	5	5	3
Average	34.6	39	16.8	4.4	3.2	2

The aerodynamic diameter ranges for particles collected by the impactor stages are: stage 6, $< 0.25\mu m$; stage 5, $0.25\mu m$ to $0.5\mu m$; stage 4, $0.5\mu m$ to $1\mu m$; stage 3, $1\mu m$ to $2\mu m$; stage 2, $2\mu m$ to $4\mu m$; stage 1, $> 4\mu m$. In general, the size distributions are biomodal with the principal mode in the fine particle range centered on stage 4 (figure 2), while the secondary maximum is not always visible. In more than 90 percent of all the particle size distributions sampled, the mass median aerodynamic diameters (i.e., half the aerosol mass was contained in diameters up to the MMAD) were $1.0\mu m$ or less. Since particles smaller than $0.1\mu m$ tend to coagulate quickly in the atmosphere to $0.1\mu m$ or larger, it can be assumed that stage 6 approximates the $0.1\mu m$ to $0.25\mu m$ diameter range. Since most of the aged atmospheric particulate sulfur lies between $0.1\mu m$ and $1.0\mu m$, as seen in figure 2, the values $0.1\mu m$, $0.5\mu m$, and $1.0\mu m$ were chosen for the calculation of b_s'.

Since, for the first case, particles of $0.1\mu m$ diameter lie in the range described by Rayleigh scattering, the formula from the Rayleigh scattering theory was used to calculate K_s.

---

[9]Robert C. West, ed., 1976, Handbook of Chemistry and Physics, Cleveland, OH, CRC Press
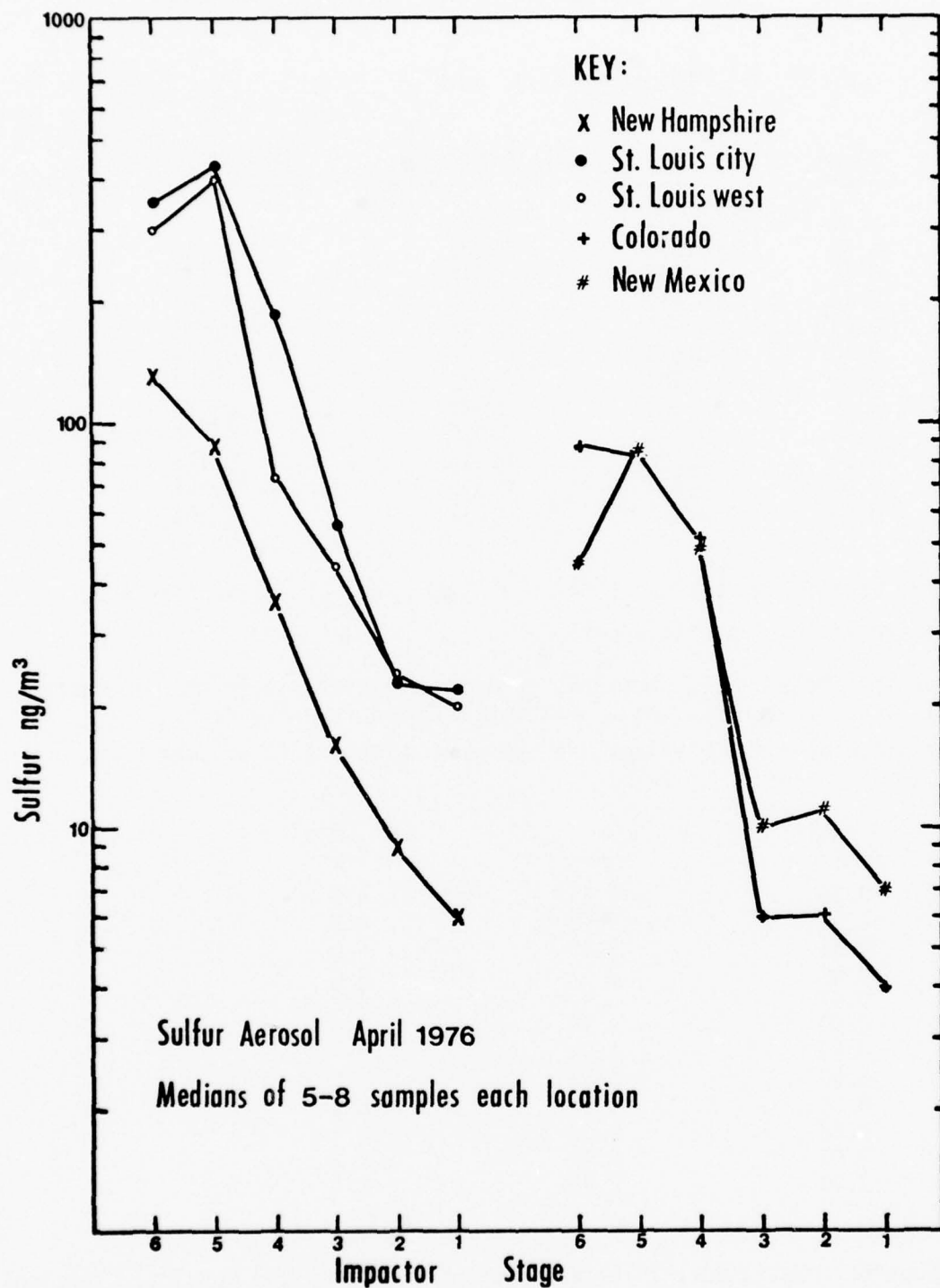
Figure 2. The size distributions of sulfur as obtained from the medians of 5-8 samples at each location as reported by J. W. Winchester (unpublished).

15

$$K_s = (8/3)X^4 \left[(m^2 - 1)/(m^2 + 2) \right]^2 \simeq 0.231X^4 \qquad (9)$$

$X = \pi D_p/\lambda$, a nondimensional optical size parameter

$m = 1.5$, the refractive index[9]

$\lambda(\mu m)$	X	K_s(Rayleigh)	P(watts $cm^{-2}\mu m^{-1}$)
0.35	0.897	0.150	0.109
0.38	0.826	0.108	0.112
0.41	0.765	0.079	0.175
0.44	0.714	0.060	0.181
0.47	0.668	0.046	0.203
0.50	0.628	0.036	0.194
0.53	0.592	0.028	0.184
0.56	0.561	0.023	0.170
0.59	0.532	0.019	0.170
0.62	0.506	0.015	0.160
0.65	0.483	0.013	0.151
0.68	0.462	0.011	0.143

From equation 8, $b_s' = 5.64 \times 10^{-13}$ cm^{-1} was calculated for a concentration of 1 particle/cm^3.

For the second case, particles of $0.5\mu m$ diameter lie in the Mie range of light scattering, and K_s was interpolated from figure 5.3 of Friedlander.[8] All P values are the same as in the first case.

$\lambda(\mu m)$	X	K_s(Mie)
0.35	4.49	4.0
0.38	4.13	4.2
0.41	3.83	4.0
0.44	3.57	4.1
0.47	3.34	3.8
0.50	3.14	3.5
0.53	2.96	3.4
0.56	2.80	3.5
0.59	2.66	2.9
0.62	2.53	2.5
0.65	2.42	2.3
0.68	2.31	2.1

[9]Robert C. West, ed., 1976, Handbook of Chemistry and Physics, Cleveland, OH, CRC Press

[8]Sheldon K. Friedlander, 1977, Smoke, Dust, and Haze, New York, Wiley

16

From equation 8, b_s' = 6.56 x 10^{-9} cm^{-1} for a concentration of 1 particle/cm^3. The third case, for aerosol particles with a diameter of 1.0μm, is again in the Mie range, and K_s was interpolated from Friedlander.[8] As before, all P values are the same as in the first case.

$\lambda(\mu m)$	X	K_s(Mie)
0.35	8.98	2.2
0.38	8.27	2.0
0.41	7.66	1.8
0.44	7.14	1.8
0.47	6.68	2.4
0.50	6.28	2.5
0.53	5.92	3.2
0.56	5.61	3.1
0.59	5.32	3.5
0.62	5.06	3.9
0.65	4.83	3.8
0.68	4.62	4.0

From equation 8, b_s' = 2.24 x 10^{-8} cm^{-1} for a concentration of 1 particle/cm^3. Using these values of b_s' for 1 particle cm^3, and a realistic concentration of atmospheric sulfate, we may calculate the overall scattering. In experimental data from this study (appendix A) sulfur concentrations as large as 6.658μg/m^3 have been observed. If the concentration of particulate sulfur is taken to be 5μg/m^3, the corresponding ammonium sulfate concentration would be approximately 20μg/m^3. Assuming this entire mass is contained in particles of a single diameter, D_p, the number of particles per cubic centimeter can be computed:

$$N\infty = \text{concentration/mass of 1 particle} \tag{10}$$

$$mass = \frac{\rho \pi D_p^3}{6} \tag{11}$$

$$\rho = 1.768 \ g/cm^3$$

---

[8]Sheldon K. Friedlander, 1977, Smoke, Dust, and Haze, New York, Wiley

D_p, μm	N_∞, particles/cm^3
0.1	21.6×10^3
0.5	1.728×10^2
1.0	2.16×10^1

For example, for a 20μg/m^3 concentration of $(NH_4)_2SO_4$ dispersed uniformly into particles of these three sizes, the scattering coefficient b_s' becomes:

D_p, μm	b_s', cm^{-1}
0.1	1.219×10^{-8}
0.5	1.13×10^{-6}
1.0	4.84×10^{-7}

To calculate visibility, the light scattered by air molecules should be included. So for air molecules with $\bar\lambda$(0.35μm to 0.7μm), b_{mol} = 2.53×10^{-7} cm^{-1}.[8] Adding this value to the previous values for b_s', the following values of b_s are obtained for a monodisperse aerosol of 20μg/m^3 of $(NH_4)_2SO_4$ of each of the three particle diameters:

D_p, μm	b_s', cm^{-1}
0.1	2.65×10^{-7}
0.5	1.38×10^{-6}
1.0	7.37×10^{-7}

For a more realistic aerosol, approximately that shown in figure 2, we may use the above calculated b_s' values for the 0.1μm, 0.5μm, and 1.0μm diameter particles in a rough calculation of visibility, if these b_s values are taken to represent impactor stages 6, 5, and 4, respectively (figure 2), with the appropriate percentage size distribution correction.

Starting with a total ammonium sulfate concentration of 20μg/m^3, the following results are obtained:

---

[8]Sheldon K. Friedlander, 1977, <u>Smoke</u>, <u>Dust</u>, <u>and Haze</u>, New York, Wiley

Stage	b_s', cm^{-1}, for 1 particle/cm^3	Concentration, μg/m^3
6	5.64×10^{-13}	6.92
5	6.56×10^{-9}	7.8
4	2.24×10^{-8}	3.36

Stage	Particle/cm^3	b_s', cm^{-1}
6	7.47×10^3	4.213×10^{-9}
5	6.74×10^1	4.421×10^{-7}
4	3.63×10^0	8.128×10^{-8}

For all three size ranges, b_s' (total) = 4.213×10^{-9} + 4.421×10^{-7}
8.128×10^{-8} = 5.276×10^{-7} cm^{-1}. To include Rayleigh scattering by air
molecules, b_{mol} = 2.53×10^{-7} cm^{-1} (Friedlander[8]) is added to the above
b_s' (total) value for the overall extinction coefficient:

$$b_s' + b_{mol} = 7.806 \times 10^{-7} \text{ cm}^{-1} = 7.806 \times 10^{-5} \text{ m}^{-1} . \tag{12}$$

Using $S = 3.912/b_{ext}$[8] to calculate visibility gives the following result:

$S = 50$ km $\rightarrow$ 31 mi.

The above result is the theoretical visual range possible with the assumption
that the relative humidity is less than 70 percent. Since relative humidities
frequently exceed 70 percent during early morning hours, the effects of high
relative humidity need to be considered. Figure 3[10] is an experimental re-
sult of b_s at different relative humidities normalized to b_s at a relative

humidity of 20 percent. The graph indicates that at relative humidity =
75 percent, b_s begins to increase drastically, and by relative humidity =

90 percent, b_s is 3.5 times the value at relative humidity = 20 percent.

Thus, at a relative humidity of 90 percent, the visibility would be reduced
by a factor of 3.5; i.e., a visibility of 50 km (31 mi) is reduced to 14 km
(9 mi). As relative humidity approaches 100 percent, visibility obscuration,
due to ammonium sulfate haze alone, can be expected to drop below 5 km
(before fog formation). Any additional atmospheric particles would reduce
visibility still further.

---

[8]Sheldon K. Friedlander, 1977, Smoke, Dust, and Haze, New York, Wiley

[10]Samuel S. Butcher and Robert J. Charlson, 1972, An Introduction to Air
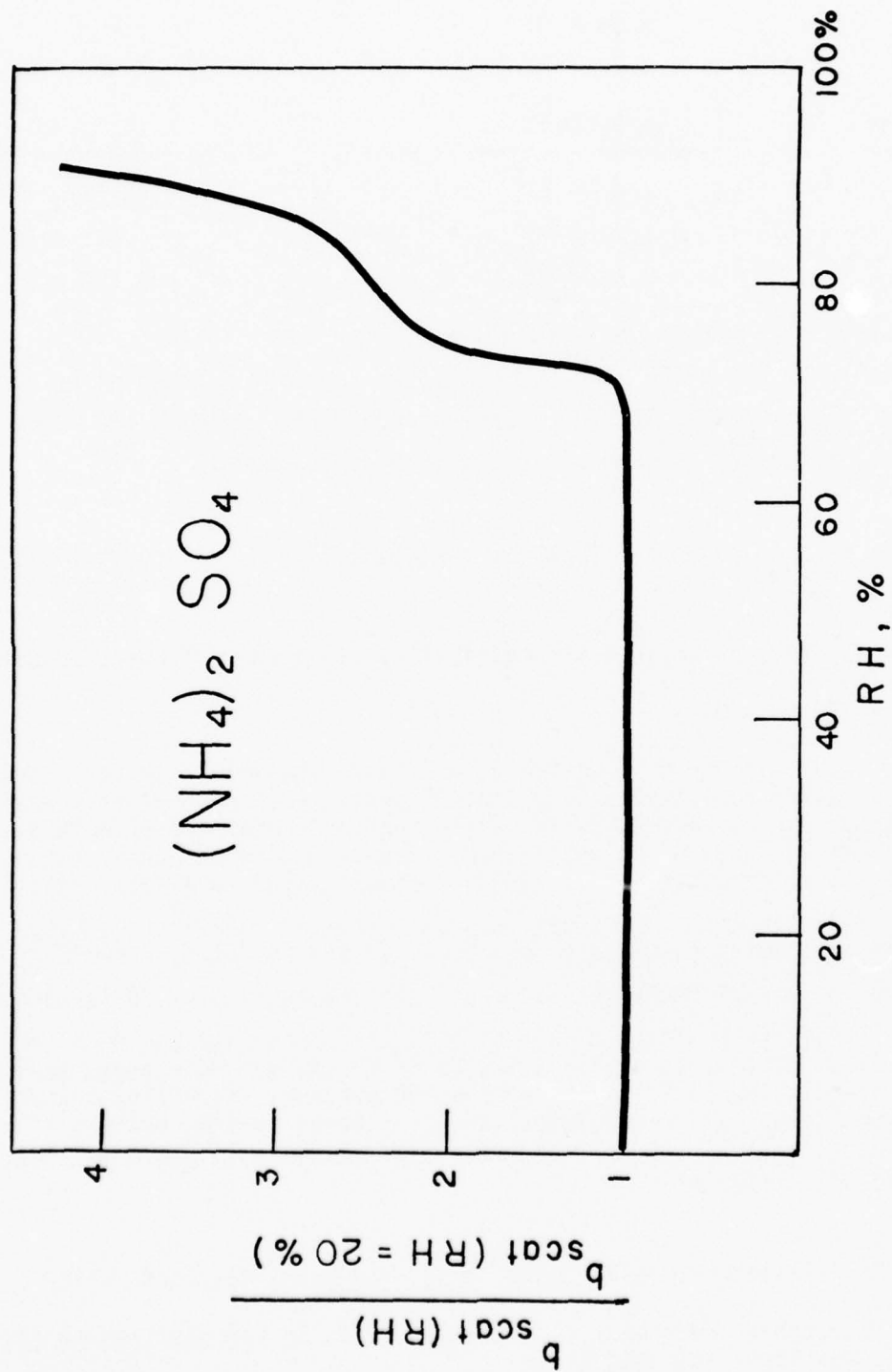Chemistry, New York, Academic Press

Figure 3. The $(NH_4)_2SO_4$ light scattering coefficient (b_{scat}) at varying relative humidities normalized to the b_{scat} value at a relative humidity of 20%.

EXPERIMENTAL

The calculations in the theoretical section were based on an ammonium sulfate concentration which was comparable to sulfur concentrations observed in this and past studies. The instrument used in sampling the atmospheric sulfur particulates, known as a streaker (invented by Nelson in 1977), has a continuous 1-week sampling capability and a temporal resolution of 2 hours. With this fine time resolution allowed by the streaker, short-lived meteorological phenomena can be studied in relation to the time variation of atmospheric sulfur particulates. A 14-station, 17-sampler network employing the streaker was initiated in June 1976 covering a wide area in the Midwestern and Northeastern United States as seen in figure 4 (upper) and table 2; meteorological data from nearby stations (figure 4 (lower) and table 3) were used in the interpretation.

The analysis technique used in this study is known as PIXE, Proton Induced X-ray Emission.[11] The sample, which is on a Nuclepore filter, is placed in a vacuum chamber and irradiated by a five million electron-volt proton beam. This beam excites the various elements in the sample and causes them to emit X-rays which are characteristic of the various elements. By "counting" the number and strength of the X-rays given off by the sample, an elemental spectrum is constructed. The sensitivity of this analysis technique allows elemental concentrations down to the nanogram range to be measured.

Since this analysis technique is sensitive for elements independent of their state of chemical combination, other information was acquired to determine which compounds are present in the sample. Since high sulfate levels have been documented during periods of low visibility,[1] extensive meteorological data were acquired from the National Climatic Center for 44 first-order meteorological stations as shown in figure 4 (lower). Specifically, visibility, precipitation, relative humidity, windspeed, and wind direction were of primary interest. Visibility was chosen because of the earlier documentation of low visibility during periods of high sulfate concentrations.[1] Precipitation is important as it is the single most efficient means of removing suspended particulates from the atmosphere.[12] Relative humidity in excess of 70 percent has been shown to be associated with reduced visibility[12] and therefore must be considered. Windspeed and wind direction are of obvious importance in the transport and dispersion of particulates in the atmosphere.

---

[11]T. B. Johansson et al., 1975, "Elemental trace analysis of small samples by proton induced X-ray emission," Anal Chem, 47:855-860

[1]R. B. Husar et al., 1976, "Long range transport of pollutants observed through visibility contour maps, weather maps, and trajectory analysis," Third Symposium on Atmospheric Turbulence, Diffusion, and Air Quality, given by the American Meteorological Society on 19-22 October, 1976, Raleigh, NC, 344-347

[12]C. E. Junge, 1963, Air Chemistry and Radioactivity, New York and London, Academic Press

21
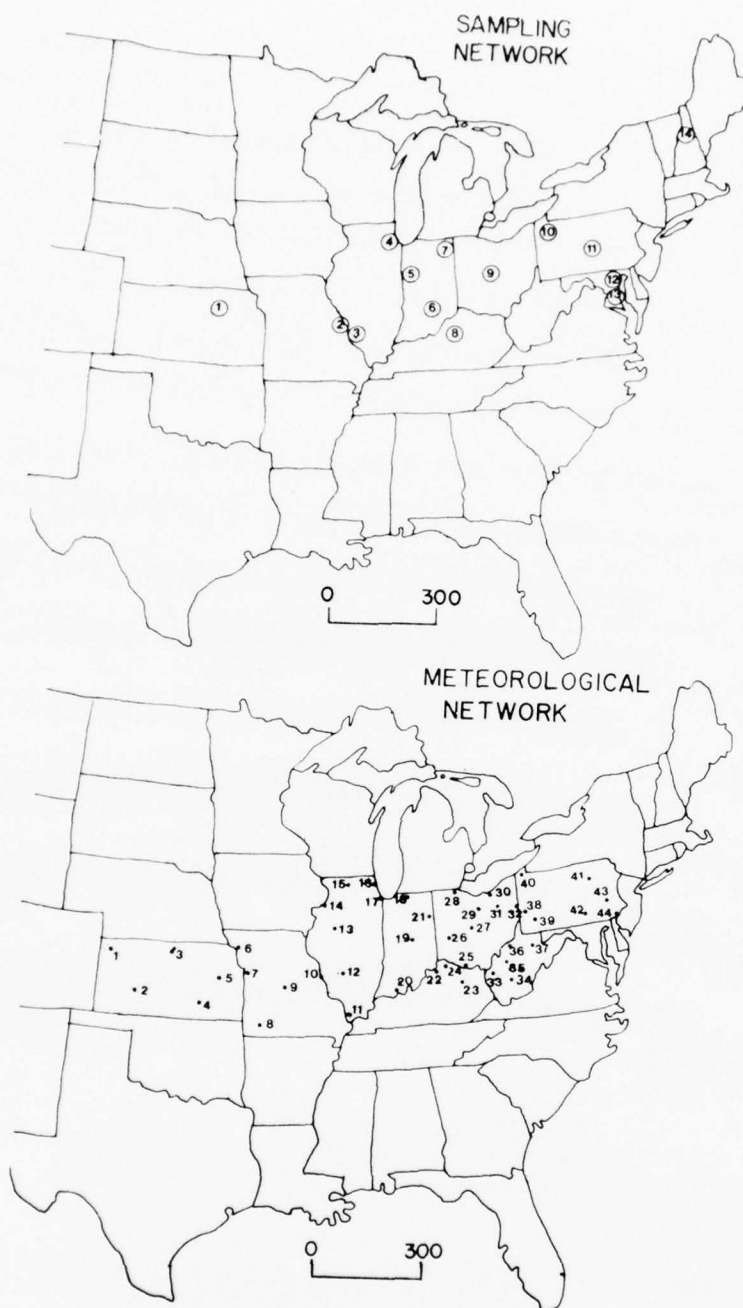
Figure 4.   (Upper) the 14 aerosol sampling sites.
            (Lower) the 44 first order meteorological stations.

22

TABLE 2. SAMPLING NETWORK

Station Number	Station Name
1	Manhattan, KS
2	Saint Louis, MO
3	Saint Louis, MO
4	Argonne, IL
5	Remington, IN
6	Morgan-Monroe State Forest, IN
7	Pokagon State Park, Angola, IN
8	Frankfort, KY
9	Delaware, OH
10	Meadville, PA
11	University Park, PA
12	Annapolis, MD
13	Annapolis, MD
14	West Thornton, NH

TABLE 3. METEOROLOGICAL NETWORK

Station Number	Station Location
1	Goodland, KS
2	Dodge City, KS
3	Concordia, KS
4	Wichita, KS
5	Topeka, KS
6	Saint Joseph, MO
7	Kansas City, MO
8	Springfield, MO
9	Columbia, MO
10	Saint Louis, MO
11	Cairo, IL
12	Springfield, IL
13	Peoria, IL
14	Moline, IL
15	Rockford, IL
16	Chicago, IL (Midway)
17	Chicago, IL (O'Hare)
18	South Bend, IN
19	Indianapolis, IN
20	Evansville, IN
21	Fort Wayne, IN
22	Louisville, KY
23	Lexington, KY
24	Greater Cincinnati Airport, OH
25	Cincinnati, OH
26	Dayton, OH
27	Columbus, OH
28	Toledo, OH
29	Mansfield, OH
30	Cleveland, OH
31	Akron, OH
32	Youngstown, OH
33	Huntington, WV
34	Beckley, WV
35	Charleston, WV
36	Parksburg, WV
37	Elkins, WV
38	Pittsburgh, PA (International Airport)
39	Pittsburgh, PA (Federal Bldg)
40	Erie, PA
41	Williamsport, PA
42	Harrisburg, PA
43	Allentown, PA
44	Philadelphia, PA

DATA ANALYSIS AND DISCUSSION

Streaker samplers were run at nonurban sampling stations 1, 2, 4, 5, 7, 9, and 10 during the period of 17-24 July 1976. Details of aerosol sampling conditions at each station have been given by Berg et al.[13,14] and Vie le Sage et al.[15] Figures 4 and 5 show the sampling network and the period of time the samplers ran at each station, respectively. Station-to-station distances ranged from 150 km between stations 4 and 5 to as much as 550 km between stations 1 and 2. July 19-20, 1976, was chosen as the period of interest because there were seven sampling stations in simultaneous operation and the meteorological conditions were favorable for large increases in the particulate pollution.

Network Meteorological Conditions

Figures 6 and 7 illustrate the surface synoptic conditions from 0000 CST, 19 July through 1800 CST, 20 July 1976. These maps were adapted from National Weather Service surface facsimile charts. During this period the surface wind flow was dominated by a large anticyclone located along the middle Atlantic coast initially, which later combined with the Bermuda anticyclone. Under these conditions winds were light and variable during the late night and early morning on 19 July in the eastern one-third of the network. The remainder of the network had light south to southwest wind flow. As a weak cool front approached the network from the northwest on 20 July, the wind flow became moderate from a south to southwest direction over the entire network. No significant precipitation was reported until late on 20 July when an instability line preceding the cool front caused some showers and thundershowers in northern Illinois and Indiana.

The 850 mb surface showed little directional or speed shear with surface wind observations. In addition, radiosonde stations located throughout the network indicated that virtually the entire network from Missouri east to Pennsylvania had an inversion between 750 mb and 850 mb on 19 and 20 July 1976. This pattern would favor long-range transport of atmospheric particulates with a depth of about 1500 to 2400 m.

---

[13]W. W. Berg et al., 1977, "Hourly variation of aerosol composition in the Great Lakes Basin," J of Great Lakes Res, 278-290

[14]W. W. Berg et al., 1977, "Time dependent sulfur and trace metal correlations in nonurban aerosols from an eastern US mesoscale network," AICHE 70th Annual Meeting, New York

[15]R. Vie le Sage et al., 1978, "Variation de la composition chimque des aerosols atmospheriques en fonction du temps," Pollution Atmospherique, 77:6-16
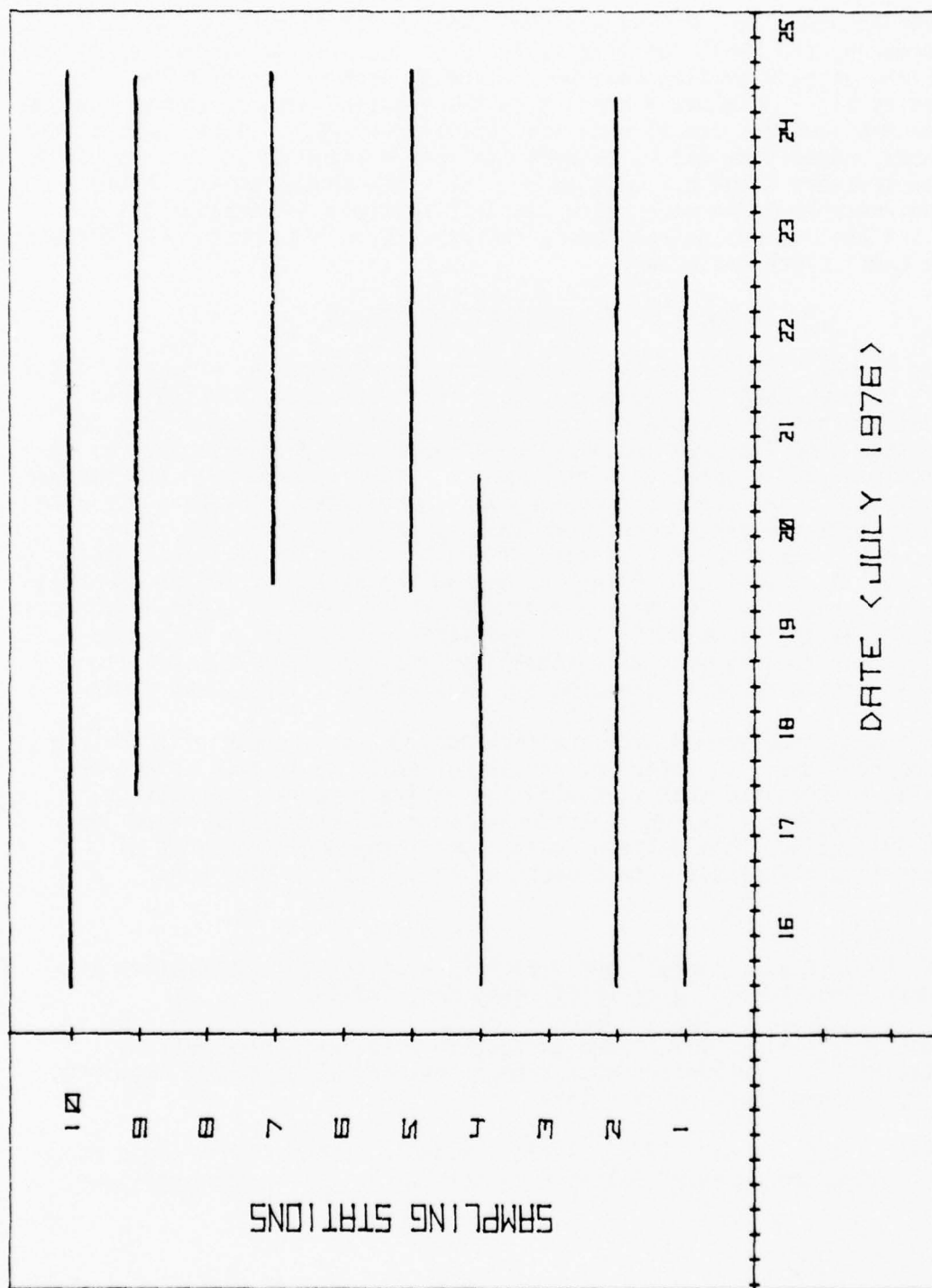
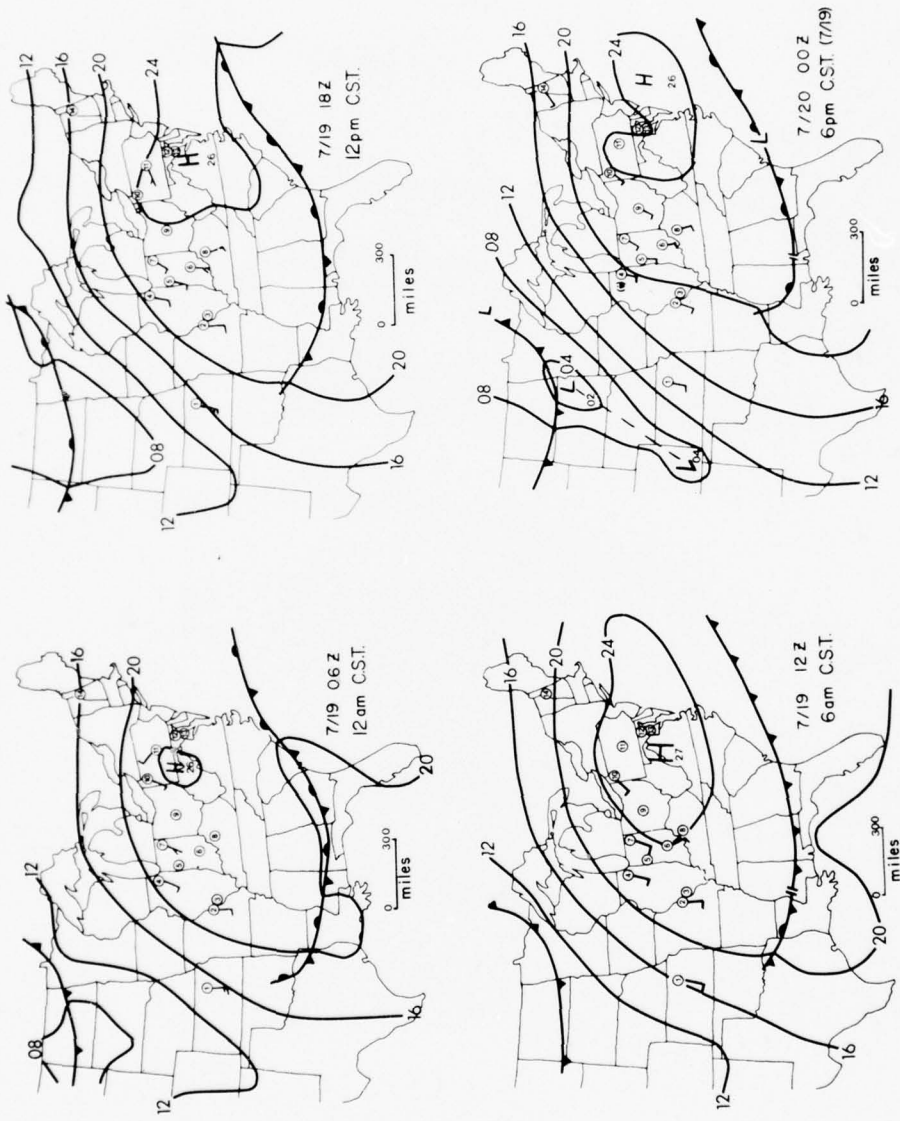Figure 5. The aerosol sampling times of the 7 sampling stations operating between July 15-25, 1976.

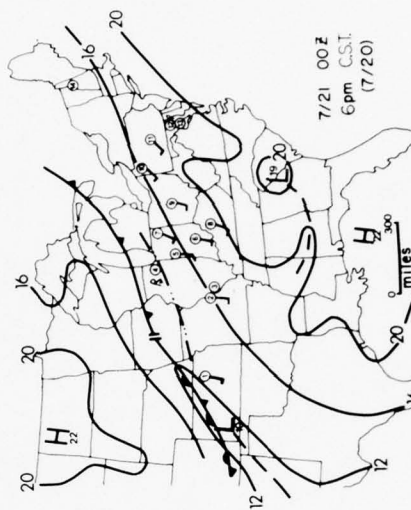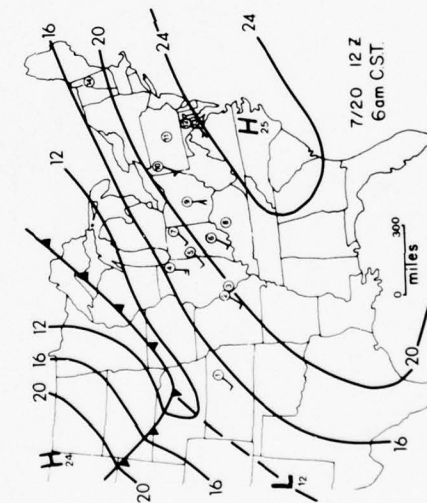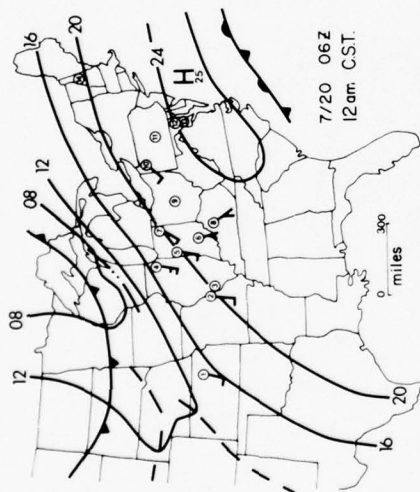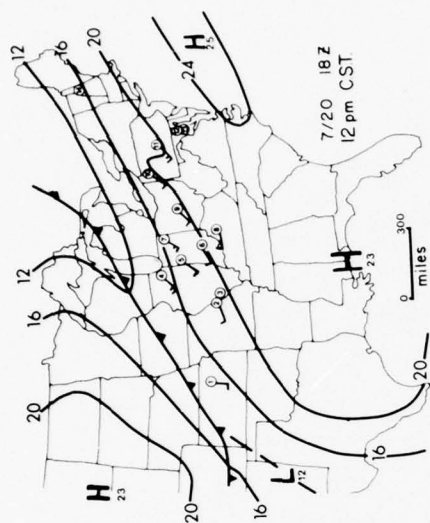Figure 6. The synoptic weather conditions on July 19, 1976.

27

Figure 7. The synoptic weather conditions on July 20, 1976.

Network Sulfur and Haze Data and Discussion

On the morning of 19 July, network sulfur concentrations over $3\mu g/m^3$ of air were found in the Illinois-Missouri area (figure 8). The $3\mu g/m^3$ isopleth extended northeast from Saint Louis into central Illinois. Most of Illinois including the Chicago and Saint Louis metropolitan areas had $2\mu g/m^3$. The remainder of the network had values generally below $1\mu g/m^3$ except for Meadville, Pennsylvania, and the Ohio River Valley. On the following morning, at the same time, network sulfur values had increased by more than two-fold over most areas. Concentrations of $2\mu g/m^3$ covered all or part of Missouri, Illinois, Indiana, Ohio, Pennsylvania, and Kentucky (figure 8). Maxima greater than $4\mu g/m^3$ appeared in northeastern Illinois and northern Indiana along with a $3\mu g/m^3$ maximum in northwestern Pennsylvania.

Haze observations were of interest during this period of dramatic increases in particulate sulfur concentrations. Haze, as defined by the National Weather Service, is a suspension in the air of extremely small dry particles invisible to the naked eye and sufficiently numerous to give the air an opalescent appearance. Figure 9 illustrates those stations reporting haze (black area) on 19 July. The numbers at the various stations outside the black area indicate the visibility in miles. Inside the black area, visibility was less than 7 mi. The haze area on 19 July grew slightly through the morning hours but essentially remained unchanged. Visibilities outside the haze regions were generally 10 mi or greater except at 0600 CST when some values between 7 and 10 mi were reported. On the morning of 20 July (figure 10), there were three small areas and one large area of haze. As the day progressed the large area of haze, which extended from northern Illinois into West Virginia, expanded northeastward. By 0300 CST the main haze area covered northeastern Illinois, northern Indiana, most of Ohio, and western West Virginia. A dramatic increase in haze occurred between 0300 CST and 0600 CST. The large area of haze expanded along with two smaller areas along the Mississippi and Ohio Rivers, until Illinois, Indiana, Ohio, northern Kentucky, western Pennsylvania, and western West Virginia were covered by haze. Visibilities outside the haze area were generally 7 to 10 mi except in Missouri and Kansas where 12 to 20 mi was common. The rapid increase in haze reported coincides with the dramatic increase in sulfur concentrations. Since relative humidities were below 100 percent on both mornings in the haze areas, as seen in figure 11, fog was not considered a factor in the reporting of haze. However, relative humidities were generally over the 80 percent figure on both mornings over a large portion of the network. The facts suggest a possible correlation between the occurrence of haze (visibility obscuration) and high particulate sulfur concentrations. There is also a suggestion that relative humidity plays an important role in the formation of haze.

In an attempt to verify that high relative humidity enhances the light scattering capabilities of ammonium sulfate, a linear regression was done on data from sampling sites 4, 9, and 10 which were considered to be the clearest examples of the above hypothesis. The data were divided into two
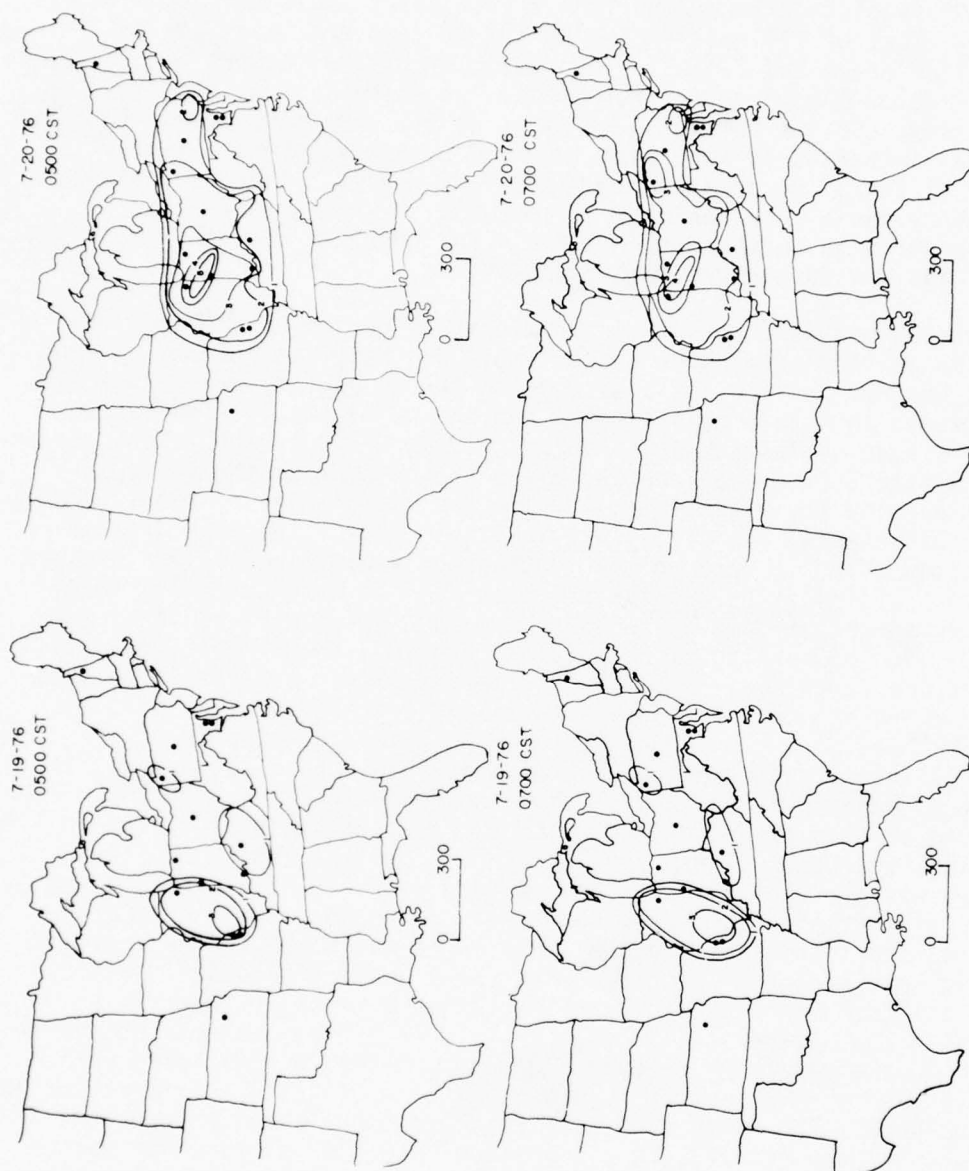
Figure 8.   Network sulfur concentration values on the mornings of July 19 and 20. Isopleths are labeled in micrograms per cubic meter.

7-20-76
0500 CST

7-20-76
0700 CST

7-19-76
0500 CST

7-19-76
0700 CST

300

300

300

300
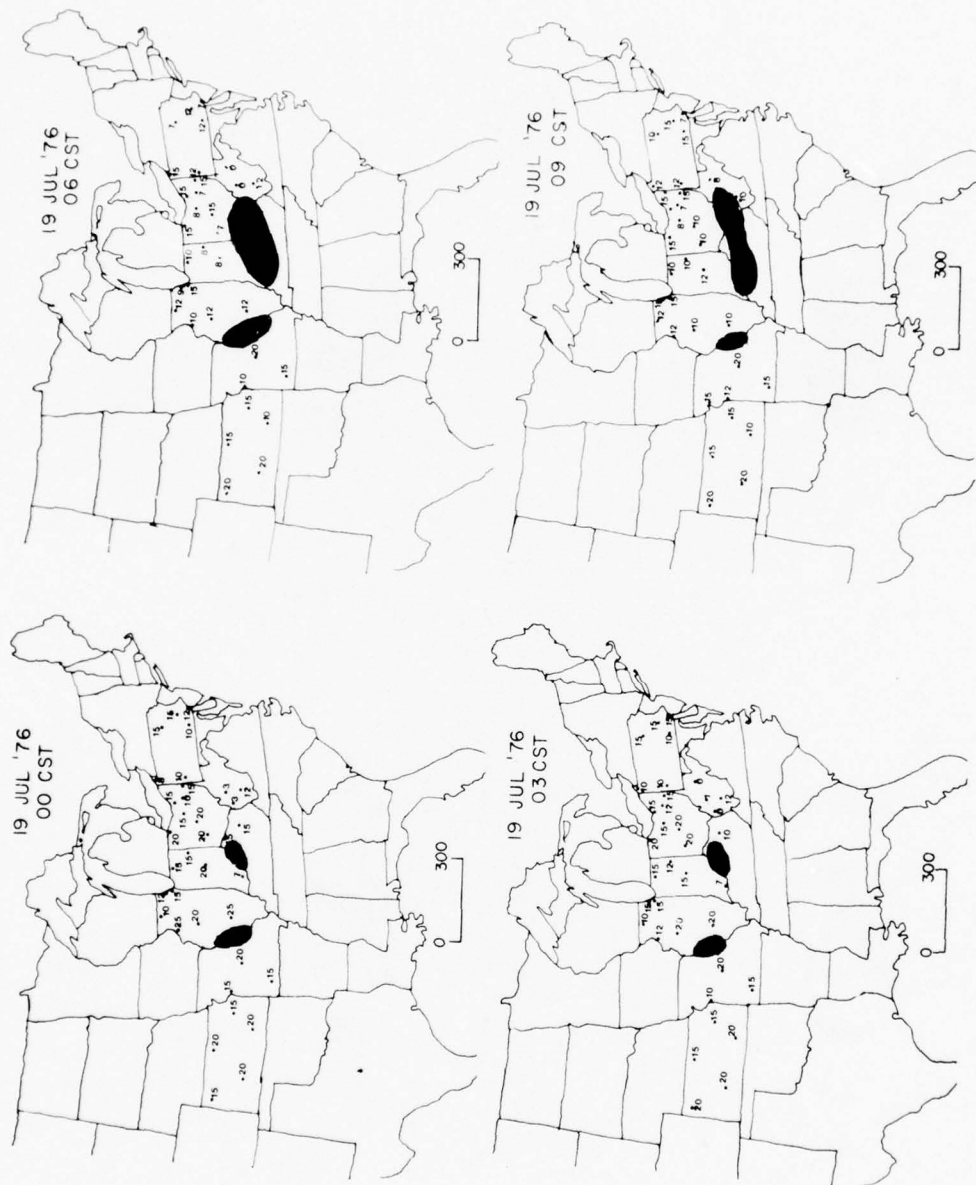
Figure 9. Visibility (numbers) in miles and reported haze (shaded area) on the morning of July 19.

31
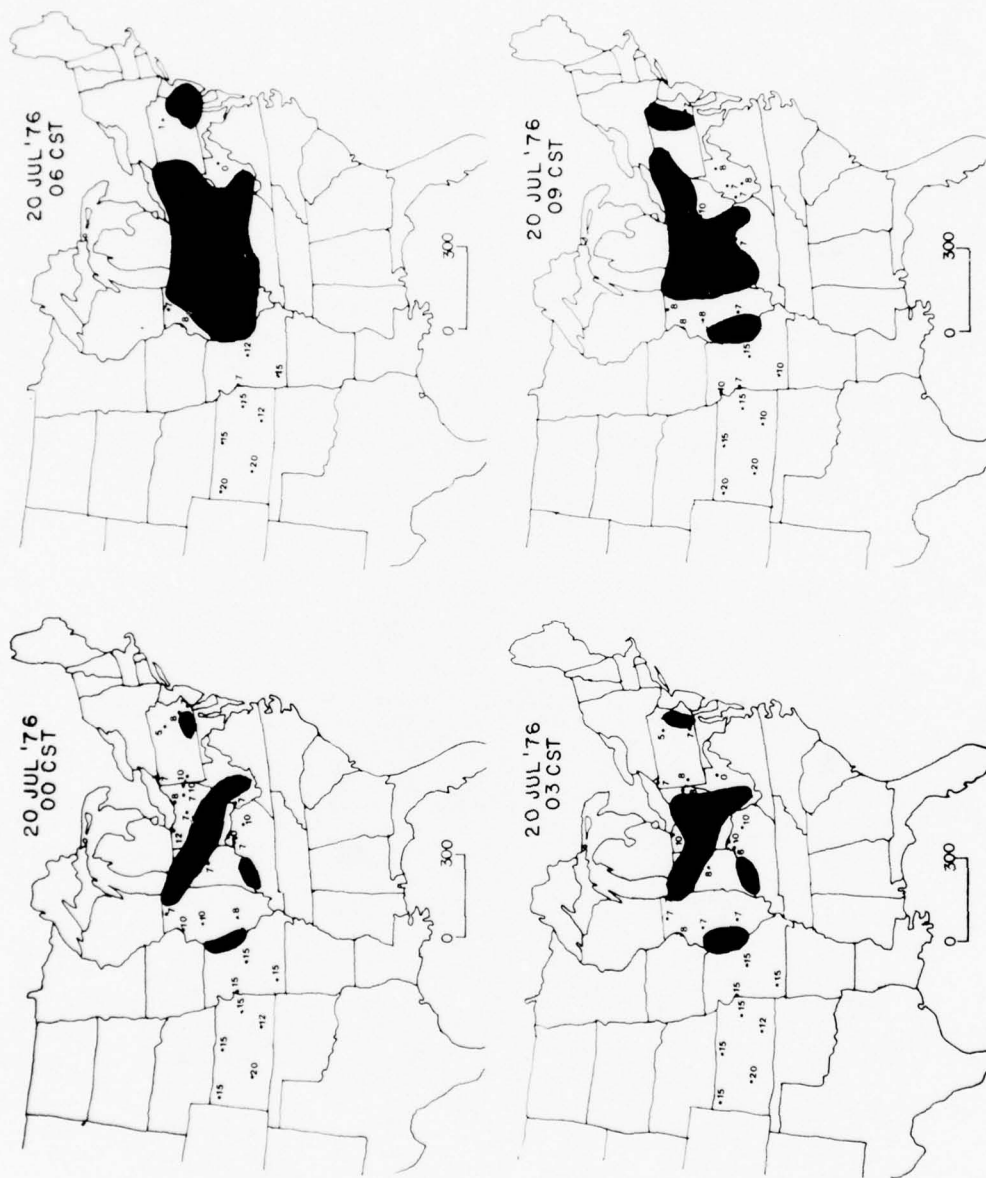
Figure 10. Visibility (numbers) in miles and reported haze (shaded area) on the morning of July 20.

32
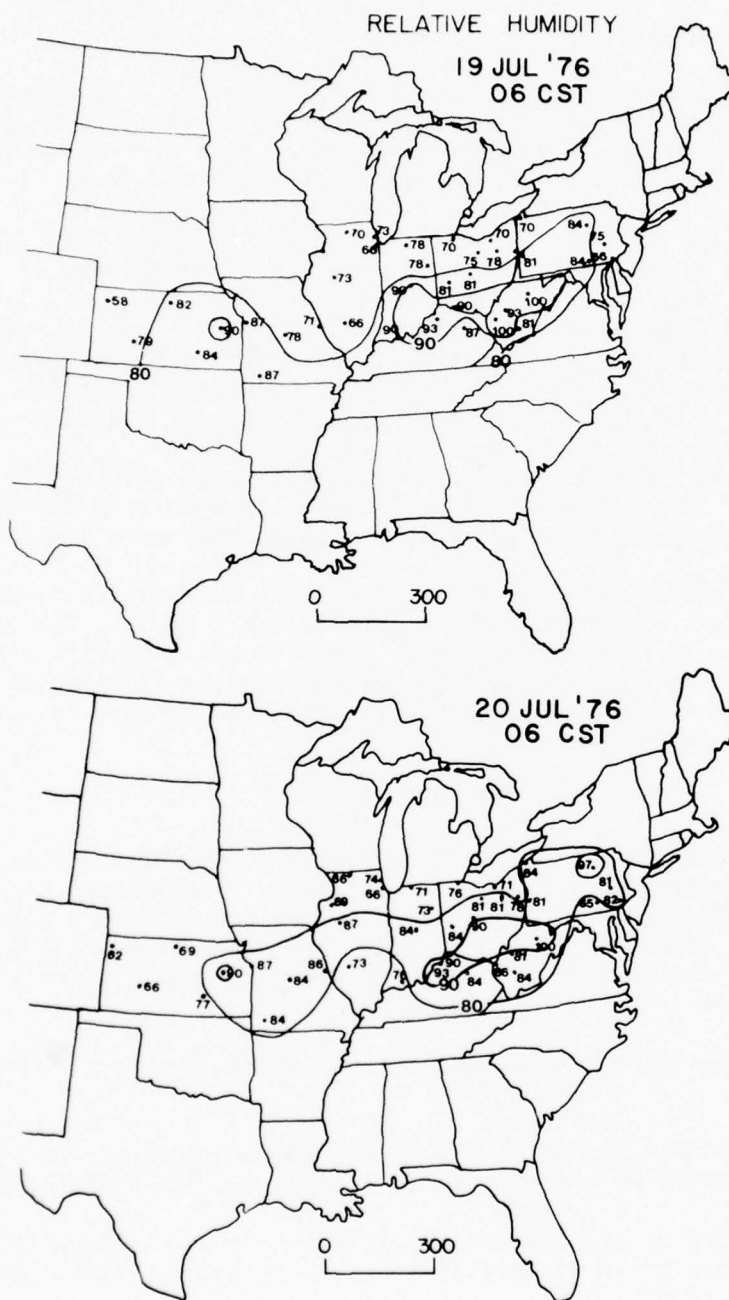
Figure 11. Network relative humidities with 80% and 90% isopleths on the mornings of July 19 and 20.

33

relative humidity groups consisting of a low group (< 70 percent) and a high group (≥ 80 percent). The computations for the low relative humidity group gave a correlation coefficient of 0.74, while the correlation co-efficient for the high relative humidity group was 0.73. A 95 percent confidence level was chosen to test both coefficients, and both results were found to be significant at this level.

These linear regression results indicate that there is a correlation between high ammonium sulfate levels and reduced visibility at both low and high relative humidities. Although there is no real difference between the correlation coefficients for the two humidity groups, this does not indicate that high relative humidity fails to enhance the visibility reducing capabilities of ammonium sulfate. Figure 12 shows the scatter diagram of sites 4, 9, and 10 for both relative humidity groups. In the low relative humidity group, visibilities of 6 mi or less are reached at ammonium sulfate concentrations of $3\mu g/m^3$ and higher. But in the high relative humidity group, the threshold of a 6-mi visibility range is at $0.8\mu g/m^3$. This strongly indicates that high relative humidities significantly enhance the visibility reducing capabilities of ammonium sulfate.

These results verify the modeling done in the theoretical section. Both the modeling and the above regression results agree on both the low and high humidity correlation coefficient results as they were discussed above.

The maximum visibility observed at all stations, except site 2, was between 15 and 20 mi, while the maximum at site 2 was 12 mi. The theoretical minimum visibility calculated previously was 9 mi with a $20\mu g/m^3$ concentration of sulfate, indicating ammonium sulfate is reducing visibility as much as 40 percent to 55 percent once the aerosol is activated by high relative humidity.

CONCLUSIONS

The temporal resolution of the streaker has proved to be essential in this study. Since the frequency of the concentration observations was nearly the same as the frequency of the meteorological observations, direct comparisons between both data sets were possible. These comparisons allowed the investigation of short-term variations in both data sets, which yielded the following results:

1. The sulfur aerosol examined in this study is primarily ammonium sulfate.

2. Relative humidity in excess of 80 percent enhances the visibility reducing capabilities of ammonium sulfate by as much as a factor of four.

3. High ammonium sulfate concentrations are correlated with reduced visibility as compared to visibilities during periods of low ammonium sulfate concentrations.

4. The large area of haze which formed on the morning of 20 July was due in large part to the combination of high ammonium sulfate levels

34
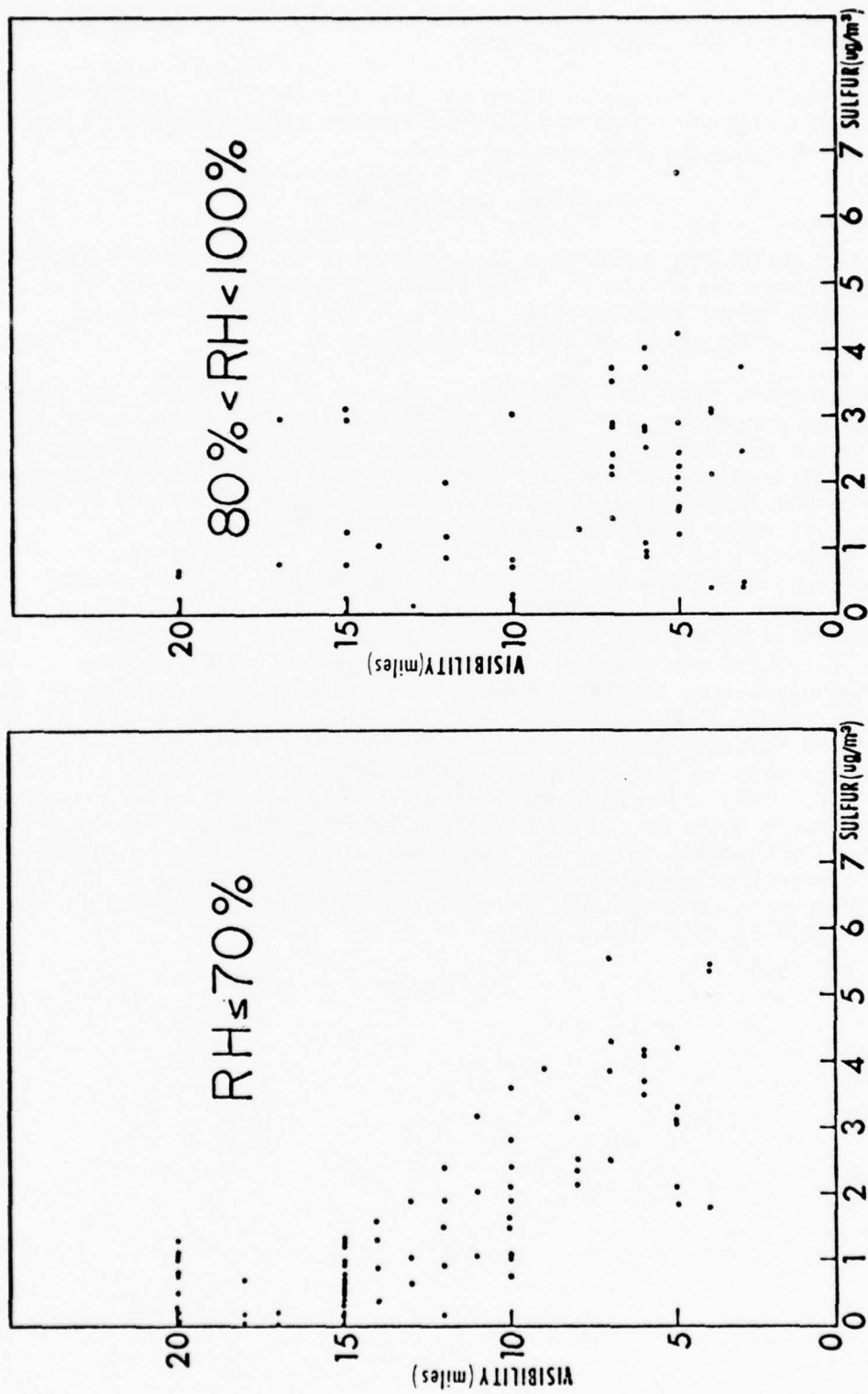
Figure 12. Scatter diagrams of sulfur concentration ($\mu g/m^3$) vs visibility (miles) at low and high relative humidities at sites 4, 9, and 10.

35

along with the high relative humidity levels which were prevalent over a large portion of the sampling network.

5.   There is a threshold value of relative humidity, approximately 81 percent, which when combined with sufficient concentrations of ammonium sulfate will cause the formation of haze.

MILITARY APPLICATION

The above conclusions as related to battlefield obscuration are significant. *If a haze formation occurs over the battlefield, the reduction in visibility could hamper both airborne observation platforms and those weapon systems dependent on the visible spectrum.*

Even though this study was done in the Eastern United States, the results are applicable over most of the globe, especially in the midlatitudes of the European continent. The highly industralized areas of Northwest Europe along with the prevailing westerly wind flow at most of the lower layers of the atmosphere, as well as the cool and moist nature of the climate, all favor the formation of hazes and fogs.

Although this study was centered only on the visible portion of the spectrum, there is an implication that the near infrared portion of the spectrum could be affected in a similar manner since 26.4 percent of the sulfate collected was $\geq 0.5\mu m$ as shown in figure 2. This in turn could disable those weapon systems designed to operate in this portion of the spectrum. There is a further suggestion, since much of the ammonium sulfate was in solution (droplets), that the absorption characteristics of fog and wet haze may be altered from those of pure water. This in turn could affect many infrared weapon systems now being developed or used. If this proves to be true, it could greatly alter the commander's decision on weapons deployment in a given situation. Although this is speculation, there is enough evidence here to suggest that further study on the effects that atmospheric ammonium sulfate could have on present and future weapon systems would be profitable.

36

REFERENCES

1. Husar, R. B., N. V. Gillani, J. D. Husar, C. C. Ailey, and P. N. Tureu, 1976, "Long range transport of pollutants observed through visibility contour maps, weather maps, and trajectory analysis," Third Symposium on Atmospheric Turbulence, Diffusion, and Air Quality, given by the American Meteorological Society on 19-22 October 1976, Raleigh, NC, 344-347.

2. Tong, E. Y., G. M. Hidy, T. F. Lavery, and F. Berland, 1976, "Regional and local aspects of atmospheric sulfates in the northeast quadrant of the United States," Third Symposium on Atmospheric Turbulence, Diffusion, and Air Quality, given by the American Meteorological Society on 19-22 October 1976, Raleigh, NC, 307-310.

3. Williamson, S. J., 1973, Fundamentals of Air Pollution, Reading MA, Addison-Wesley Publishing Company, 472 pp.

4. Ehrlich, P. R., Anne H. Ehrlich, and John P. Holdren, 1977, Ecoscience, San Francisco, W. H. Freeman and Company, 1051 pp.

5. Sawyer, J. W., 1978, "The sulfur we breathe," Environment, 20:25-26.

6. Ahlberg, M. S., A. C. D. Leslie, and J. W. Winchester, 1978, "The chemical state of particulate sulfur in ambient aerosols determined by PIXE analysis," Nucl Instr and Meth, 149:451-455.

7. US Environmental Protection Agency, 1975, Position paper on regulation of atmospheric sulfates, EPA-450/2-75-007, Research Triangle Park, NC.

8. Friedlander, Sheldon K., 1977, Smoke, Dust, and Haze, New York, Wiley, 317 pp.

9. West, Robert C., ed., 1976, Handbook of Chemistry and Physics, Cleveland, OH, CRC Press.

10. Butcher, Samuel S., and Robert J. Charlson, 1972, An Introduction to Air Chemistry, New York, Academic Press, 241 pp.

11. Johansson, T. B., R. E. Van Grieken, J. W. Nelson, and J. W. Winchester, 1975, "Elemental trace analysis of small samples by proton induced X-ray emission," Anal Chem, 47:855-860.

12. Junge, C. E., 1963, Air Chemistry and Radioactivity, New York and London, Academic Press, 382 pp.

13. Berg, W. W., R. Vie le Sage, K. Sato, J. O. Pilotte, S. L. Cohn, J. W. Winchester, and J. W. Nelson, 1977, "Hourly variation of aerosol composition in the Great Lakes Basin," J of Great Lakes Res, 278-290.

14. Berg, W. W., K. Sato, R. Vie le Sage, J. W. Winchester, and S. L. Cohn, 1977, "Time dependent sulfur and trace metal correlations in nonurban aerosols from an eastern US mesoscale network," AICHE 70th Annual Meeting, New York.

15. Vie le Sage, R., W. W. Berg, S. L. Cohn, J. W. Winchester, and J. W. Nelson, 1978, "Variation de la composition chimque des aerosols atmospheriques en fonction du temps," Pollution Atmospherique, 77:6-16.

SULFUR CONCENTRATIONS IN NANOGRAMS PER CUBIC METER FOR THE PERIOD
OF 15 THROUGH 24 JULY 1976

Zero indicates a value below the detection limit. Data columns are matched with
those of appendix B. Sulfur data in column 6, appendix A, were taken near the
station which gave the weather data in column 6, appendix B.

SULFUR CONCENTRATION (ng/m^3)

DATE	HOUR	STATION NUMBER						
		1	2	4	5	7	9	10
7-15	1200	102	332	451				3138
	1400	231	249	585				1939
	1600	164	278	560				2112
	1800	75	370	426				2145
	2000	44	338	685				1836
	2200	73	422	668				1554
7-16	0000	78	389	525				1670
	0200	68	498	377				1335
	0400	42	515	385				1396
	0600	67	624	389				1673
	0800	147	535	186				1955
	1000	113	692	161				2461
	1200	40	754	77				2385
	1400	50	501	132				2331
	1600	38	411	262				2213
	1800	66	439	244				796
	2000	117	591	245				210
	2200	118	680	254				230
7-17	0000	133	907	229				116
	0200	143	545	175				216
	0400	128	660	0				255
	0600	147	1029	67				126
	0800	108	936	0				234
	1000	94	1375	6			202	628
	1200	99	756	95			297	595
	1400	0	1076	49			504	938
	1600	24	1825	9			765	703
	1800	88	2133	69			774	779
	2000	201	1667	57			1062	1213
	2200	766	1522	17			1120	1412
7-18	0000	935	1430	0			2957	1318
	0200	399	1463	40			2955	1294
	0400	243	1625	127			3106	1173
	0600	205	1782	90			3014	1170
	0800	201	2104	75			651	1040
	1000	297	3455	166			492	848
	1200	253	4269	361			686	862
	1400	239	3618	202			799	1266
	1600	266	3749	494			1290	1332
	1800	128	3704	642			807	986
	2000	169	4252	749			1018	1016
	2200	269	4104	1882			804	1100
7-19	0000	424	3609	2019			809	1187
	0200	505	5952	1984			640	1147
	0400	446	4454	2470			634	1196
	0600	380	3381	2551			756	1321
	0800	544	4545	3158			1037	1578
	1000	606	4321	3984	1402		1042	1478
	1200	546	3925	4606	3376	1958	903	1471
	1400	431	4046	3840	4908	3420	1025	2095

SULFUR CONCENTRATION (ng/m^3) -- Continued

DATE	HOUR	STATION NUMBER

DATE	HOUR	1	2	4	5	7	9	10
7-19	1600	473	4503	3677	3351	5638	1832	2804
	1800	569	4655	4264	3235	5008	2092	2517
	2000	483	3035	3899	2563	2680	3280	1816
	2200	498	2851	2110	2040	2268	2865	1274
7-20	0000	504	3198	3426	5773	2155	2784	1446
	0200	631	2772	3493	6632	4436	2822	2113
	0400	601	2139	5554	6480	4414	2460	2414
	0600	604	2012	5748	4918	2242	2110	3083
	0800	474	1821	3107	3784	2427	2068	3739
	1000	382	1377	2425	1914	2857	2390	5344
	1200	403	1014	3122	957	2630	2500	5483
	1400	374	849	2335	2513	2518	3080	1794
	1600	299	990		1702	2483	3050	4186
	1800	340	928		1414	1800	3683	4276
	2000	368	709		1185	1242	4075	3849
	2200	290	598		1643	587	3770	5306
7-21	0000	269	564		1941	685	2854	4160
	0200	377	585		1099	1281	2840	2406
	0400	409	592		818	1605	3530	2186
	0600	413	773		562	1406	2525	2683
	0800	302	618		387	1357	2426	2774
	1000	276	633		274	2349	2575	2542
	1200	260	476		517	2051	2807	2032
	1400	196	400		60	2123	2494	1844
	1600	300	290		613	1397	2036	2461
	1800	310	421		3981	1012	2228	4414
	2000	346	893		1904	701	1604	3727
	2200	240	973		1077	772	1885	2884
7-22	0000	370	1247		1271	2125	1566	1999
	0200	456	0		695	2730	1787	1250
	0400	354	0		1636	2519	1837	750
	0600	348	949		1672	2119	1533	394
	0800	263	1039		1876	1967	1126	157
	1000	308	788		2416	2261	1416	314
	1200	321	805		2102	2324	2125	527
	1400	250	35		1811	2457	2869	1289
	1600	295	453		1904	2411	2949	2392
	1800		869		1865	2701	2450	3596
	2000		764		1454	892	3045	3441
	2200		1068		1283	605	2744	4025
7-23	0000		1208		1359	748	2223	4244
	0200		1049		1439	900	856	6658
	0400		166		1327	1019	947	3385
	0600		0		1380	1080	955	1039
	0800		764		569	2109	1074	471
	1000		1259		766	2091	1215	403
	1200		788		1524	2777	1613	400
	1400		520		1310	2585	2127	879
	1600		752		1107	2076	1631	3886
	1800		1673		1116	1752	1075	5482

SULFUR CONCENTRATION (ng/m³) -- Continued

		STATION NUMBER						
DATE	HOUR	1	2	4	5	7	9	10
7-23	2000		843		1066	1816	821	5174
	2200		130		1491	1700	717	3906
7-24	0000		63		992	2080	866	2571
	0200		0		600	1671	1195	1216
	0400		739		774	1707	1386	609
	0600		2750		811	1825	1802	692
	0800		2507		829	1253	1632	847
	1000		0		702	548	964	547
	1200		0		654	460	1688	415
	1400		0		634	231	1687	485
	1600		750		525	193		715

VISIBILITY IN MILES AND RELATIVE HUMIDITY IN PERCENT FOR THE
PERIOD OF 17 THROUGH 23 JULY 1976

VISIBILITY (miles)

DATE	HOUR	STATION NUMBER						
		5	10	16	18	19	27	40
7-17	0000	15	12	20	15	20	15	10
	0300	15	10	15	15	20	15	10
	0600	10	8	15	15	4	15	15
	0900	7	12	20	12	20	20	15
	1200	15	12	20	15	20	20	15
	1500	15	12	20	15	20	20	15
	1800	15	12	20	15	20	20	15
	2100	15	12	15	15	20	20	15
7-18	0000	15	12	15	10	20	15	8
	0300	15	8	15	10	15	15	8
	0600	15	6	15	8	10	7	15
	0900	15	12	12	12	20	15	12
	1200	15	12	15	12	20	20	15
	1500	15	12	20	12	20	20	15
	1800	15	12	10	15	20	20	15
	2100	15	10	10	15	20	20	10
7-19	0000	15	8	12	15	20	20	8
	0300	15	7	15	15	15	20	10
	0600	15	6	9	10	8	15	15
	0900	15	8	15	10	12	10	12
	1200	15	8	15	10	10	12	10
	1500	15	7	12	10	7	5	10
	1800	15	6	10	10	9	5	8
	2100	10	7	5	6	8	6	8
7-20	0000	15	7	6	6	7	6	7
	0300	15	6	7	5	8	4	7
	0600	15	6	6	4	6	2	3
	0900	15	6	6	5	6	10	4
	1200	15	8	8	6	7	5	4
	1500	15	10	7	8	6	5	5
	1800	15	10	6	7	8	6	7
	2100	15	10	6	1	8	6	7
7-21	0000	15	10	4	3	10	7	5
	0300	15	8	5	4	8	7	5
	0600	15	7	1	2	7	5	1
	0900	15	8	4	2	7	3	1
	1200	15	10	8	2	6	3	1
	1500	15	10	15	6	12	3	3
	1800	15	10	20	8	12	5	7
	2100	15	10	20	10	12	5	7
7-22	0000	15	7	20	9	12	5	15
	0300	15	6	15	8	6	2	15
	0600	15	7	10	2	2	1	15
	0900	15	7	5	4	2	2	15
	1200	15	8	6	1	7	5	15
	1500	15	8	6	4	7	5	12
	1800	15	8	7	7	7	2	10
	2100	15	8	6	7	8	8	6
7-23	0000	15	10	3	4	7	6	5
	0300	15	12	3	7	10	5	4
	0600	15	8	6	7	9	7	3
	0900	15	8	7	7	10	5	3
	1200	15	10	9	7	10	7	4
	1500	15	10	10	10	15	10	2
	1800	15	12	6	7	12	10	2
	2100	15	10	10	6	10	10	3

RELATIVE HUMIDITY (%)

DATE	HOUR	STATION NUMBER						
		5	10	16	18	19	27	40
7-17	0000	97	75	62	87	96	81	75
	0300	97	87	83	90	100	83	84
	0600	97	90	78	87	100	80	93
	0900	100	46	44	53	66	59	63
	1200	97	39	37	45	48	49	59
	1500	87	41	36	37	50	46	57
	1800	66	50	37	42	46	48	70
	2100	73	63	51	70	81	70	100
7-18	0000	84	75	65	78	93	93	100
	0300	97	90	75	81	100	93	100
	0600	97	93	78	81	90	90	93
	0900	67	50	56	60	57	51	84
	1200	65	33	40	46	49	37	48
	1500	61	30	34	39	44	42	58
	1800	61	33	47	44	47	45	51
	2100	79	52	58	66	68	63	73
7-19	0000	79	64	68	76	87	84	70
	0300	84	58	73	81	97	93	78
	0600	90	71	73	76	90	81	70
	0900	77	52	54	56	69	55	60
	1200	65	45	40	47	54	52	56
	1500	63	39	48	43	53	49	64
	1800	61	48	54	58	62	54	71
	2100	74	60	79	64	84	76	84
7-20	0000	74	71	69	71	93	84	84
	0300	84	82	69	71	87	93	93
	0600	90	76	74	71	84	90	84
	0900	72	63	75	71	67	64	69
	1200	61	50	50	61	63	55	64
	1500	56	40	49	48	61	53	60
	1800	54	41	94	65	65	58	60
	2100	74	61	87	97	82	74	64
7-21	0000	67	69	97	97	82	81	93
	0300	69	85	93	97	90	84	100
	0600	82	85	100	100	90	84	100
	0900	69	65	97	93	79	74	100
	1200	65	46	79	93	61	69	100
	1500	61	44	42	65	63	87	79
	1800	61	44	50	67	72	88	81
	2100	53	77	73	76	82	93	90
7-22	0000	97	97	81	87	90	93	97
	0300	67	90	81	87	100	97	96
	0600	71	87	87	92	100	97	73
	0900	63	59	93	82	97	87	57
	1200	52	47	90	97	77	79	56
	1500	47	26	85	90	74	88	66
	1800	45	30	87	90	74	88	71
	2100	61	43	90	90	91	97	87
7-23	0000	69	58	94	97	90	97	90
	0300	74	69	90	93	87	97	93
	0600	87	76	94	97	85	97	93
	0900	61	55	79	79	67	82	85
	1200	52	39	63	70	56	65	93
	1500	49	35	59	65	49	57	97
	1800	49	40	85	58	57	82	97
	2100	77	55	82	91	88	87	100

DISTRIBUTION LIST

Dr. Frank D. Eaton
Geophysical Institute
University of Alaska
Fairbanks, AK 99701

Commander
US Army Aviation Center
ATTN: ATZQ-D-MA
Fort Rucker, AL 36362

Chief, Atmospheric Sciences Div
Code ES-81
NASA
Marshall Space Flight Center,
AL 35812

Commander
US Army Missile R&D Command
ATTN: DRDMI-CGA (B. W. Fowler)
Redstone Arsenal, AL 35809

Redstone Scientific Information Center
ATTN: DRDMI-TBD
US Army Missile R&D Command
Redstone Arsenal, AL 35809

Commander
US Army Missile R&D Command
ATTN: DRDMI-TEM (R. Haraway)
Redstone Arsenal, AL 35809

Commander
US Army Missile R&D Command
ATTN: DRDMI-TRA (Dr. Essenwanger)
Redstone Arsenal, AL 35809

Commander
HQ, Fort Huachuca
ATTN: Tech Ref Div
Fort Huachuca, AZ 85613

Commander
US Army Intelligence Center & School
ATTN: ATSI-CD-MD
Fort Huachuca, AZ 85613

Commander
US Army Yuma Proving Ground
ATTN: Technical Library
Bldg 2100
Yuma, AZ 85364

Naval Weapons Center (Code 3173)
ATTN: Dr. A. Shlanta
China Lake, CA 93555

Sylvania Elec Sys Western Div
ATTN: Technical Reports Library
PO Box 205
Mountain View, CA 94040

Geophysics Officer
PMTC Code 3250
Pacific Missile Test Center
Point Mugu, CA 93042

Commander
Naval Ocean Systems Center (Code 4473)
ATTN: Technical Library
San Diego, CA 92152

Meteorologist in Charge
Kwajalein Missile Range
PO Box 67
APO San Francisco, CA 96555

Director
NOAA/ERL/APCL R31
RB3-Room 567
Boulder, CO 80302

Library-R-51-Tech Reports
NOAA/ERL
320 S. Broadway
Boulder, CO 80302

National Center for Atmos Research
NCAR Library
PO Box 3000
Boulder, CO 80307

R. B. Girardo
Bureau of Reclamation
E&R Center, Code 1220
Denver Federal Center, Bldg 67
Denver, CO 80225

National Weather Service
National Meteorological Center
W321, WWB, Room 201
ATTN: Mr. Quiroz
Washington, DC 20233

Mil Assistant for Atmos Sciences
Ofc of the Undersecretary of Defense
    for Rsch & Engr/E&LS - Room 3D129
The Pentagon
Washington, DC 20301

Defense Communications Agency
Technical Library Center
Code 205
Washington, DC 20305

Director
Defense Nuclear Agency
ATTN: Technical Library
Washington, DC 20305

HQDA (DAEN-RDM/Dr. de Percin)
Washington, DC 20314

Director
Naval Research Laboratory
Code 5530
Washington, DC 20375

Commanding Officer
Naval Research Laboratory
Code 2627
Washington, DC 20375

Dr. J. M. MacCallum
Naval Research Laboratory
Code 1409
Washington, DC 20375

The Library of Congress
ATTN: Exchange & Gift Div
Washington, DC 20540
2

Head, Atmos Rsch Section
Div Atmospheric Science
National Science Foundation
1800 G. Street, NW
Washington, DC 20550

CPT Hugh Albers, Exec Sec
Interdept Committee on Atmos Science
National Science Foundation
Washington, DC 20550

Director, Systems R&D Service
Federal Aviation Administration
ATTN: ARD-54
2100 Second Street, SW
Washington, DC 20590

ADTC/DLODL
Eglin AFB, FL 32542

Naval Training Equipment Center
ATTN: Technical Library
Orlando, FL 32813

Det 11, 2WS/OI
ATTN: Maj Orondorff
Patrick AFB, FL 32925

USAFETAC/CB
Scott AFB, IL 62225

HQ, ESD/TOSI/S-22
Hanscom AFB, MA 01731

Air Force Geophysics Laboratory
ATTN: LCB (A. S. Carten, Jr.)
Hanscom AFB, MA 01731

Air Force Geophysics Laboratory
ATTN: LYD
Hanscom AFB, MA 01731

Meteorology Division
AFGL/LY
Hanscom AFB, MA 01731

US Army Liaison Office
MIT-Lincoln Lab, Library A-082
PO Box 73
Lexington, MA 02173

Director
US Army Ballistic Rsch Lab
ATTN: DRDAR-BLB (Dr. G. E. Keller)
Aberdeen Proving Ground, MD 21005

Commander
US Army Ballistic Rsch Lab
ATTN: DRDAR-BLP
Aberdeen Proving Ground, MD 21005

Director
US Army Armament R&D Command
Chemical Systems Laboratory
ATTN: DRDAR-CLJ-I
Aberdeen Proving Ground, MD 21010

Chief CB Detection & Alarms Div
Chemical Systems Laboratory
ATTN: DRDAR-CLC-CR (H. Tannenbaum)
Aberdeen Proving Ground, MD 21010

Commander
Harry Diamond Laboratories
ATTN: DELHD-CO
2800 Powder Mill Road
Adelphi, MD 20783

Commander
ERADCOM
ATTN: DRDEL-AP
2800 Powder Mill Road
Adelphi, MD 20783
2

Commander
ERADCOM
ATTN: DRDEL-CG/DRDEL-DC/DRDEL-CS
2800 Powder Mill Road
Adelphi, MD 20783

Commander
ERADCOM
ATTN: DRDEL-CT
2800 Powder Mill Road
Adelphi, MD 20783

Commander
ERADCOM
ATTN: DRDEL-EA
2800 Powder Mill Road
Adelphi, MD 20783

Commander
ERADCOM
ATTN: DRDEL-PA/DRDEL-ILS/DRDEL-E
2800 Powder Mill Road
Adelphi, MD 20783

Commander
ERADCOM
ATTN: DRDEL-PAO (S. Kimmel)
2800 Powder Mill Road
Adelphi, MD 20783

Chief
Intelligence Materiel Dev & Support Ofc
ATTN: DELEW-WL-I
Bldg 4554
Fort George G. Meade, MD 20755

Acquisitions Section, IRDB-D823
Library & Info Service Div, NOAA
6009 Executive Blvd
Rockville, MD 20852

Naval Surface Weapons Center
White Oak Library
Silver Spring, MD 20910

The Environmental Research
   Institute of MI
ATTN: IRIA Library
PO Box 8618
Ann Arbor, MI 48107

Mr. William A. Main
USDA Forest Service
1407 S. Harrison Road
East Lansing, MI 48823

Dr. A. D. Belmont
Research Division
PO Box 1249
Control Data Corp
Minneapolis, MN 55440

Director
Naval Oceanography & Meteorology
NSTL Station
Bay St Louis, MS 39529

Director
US Army Engr Waterways Experiment Sta
ATTN: Library
PO Box 631
Vicksburg, MS 39180

Commander
US Army Tropic Test Center
ATTN: STETC-TD (Info Center)
APO New York 09827

Commandant
US Army Field Artillery School
ATTN: ATSF-CD-R (Mr. Farmer)
Fort Sill, OK 73503

Commandant
US Army Field Artillery School
ATTN: ATSF-CF-R
Fort Sill, OK 73503

Director CFD
US Army Field Artillery School
ATTN: Met Division
Fort Sill, OK 73503

Commandant
US Army Field Artillery School
ATTN: Morris Swett Library
Fort Sill, OK 73503

Commander
US Army Dugway Proving Ground
ATTN: MT-DA-L
Dugway, UT 84022

Dr. C. R. Sreedrahan
Research Associates
Utah State University, UNC 48
Logan, UT 84322

Inge Dirmhirn, Professor
Utah State University, UNC 48
Logan, UT 84322

Defense Documentation Center
ATTN: DDC-TCA
Cameron Station Bldg 5
Alexandria, VA 22314
12

Commanding Officer
US Army Foreign Sci & Tech Center
ATTN: DRXST-IS1
220 7th Street, NE
Charlottesville, VA 22901

Naval Surface Weapons Center
Code G65
Dahlgren, VA 22448

Commander
US Army Night Vision
 & Electro-Optics Lab
ATTN: DELNV-D
Fort Belvoir, VA 22060

Commander and Director
US Army Engineer Topographic Lab
ETL-TD-MB
Fort Belvoir, VA 22060

Director
Applied Technology Lab
DAVDL-EU-TSD
ATTN: Technical Library
Fort Eustis, VA 23604

Department of the Air Force
OL-C, 5WW
Fort Monroe, VA 23651

Department of the Air Force
5WW/DN
Langley AFB, VA 23665

Director
Development Center MCDEC
ATTN: Firepower Division
Quantico, VA 22134

US Army Nuclear & Chemical Agency
ATTN: MONA-WE
Springfield, VA 22150

Director
US Army Signals Warfare Laboratory
ATTN: DELSW-OS (Dr. R. Burkhardt)
Vint Hill Farms Station
Warrenton, VA 22186

Commander
US Army Cold Regions Test Center
ATTN: STECR-OP-PM
APO Seattle, WA 98733

Dr. John L. Walsh
Code 5560
Navy Research Lab
Washington, DC 20375

Commander
TRASANA
ATTN: ATAA-PL
       (Dolores Anguiano)
White Sands Missile Range, NM 88002

Commander
US Army Dugway Proving Ground
ATTN: STEDP-MT-DA-M (Mr. Paul Carlson)
Dugway, UT 84022

Commander
US Army Dugway Proving Ground
ATTN: STEDP-MT-DA-T
       (Mr. William Peterson)
Dugway, UT 84022

Commander
USATRADOC
ATTN: ATCD-SIE
Fort Monroe, VA 23651

Commander
USATRADOC
ATTN: ATCD-CF
Fort Monroe, VA 23651

Commander
USATRADOC
ATTN: Tech Library
Fort Monroe, VA 23651

ATMOSPHERIC SCIENCES RESEARCH PAPERS

1. Lindberg, J.D., "An Improvement to a Method for Measuring the Absorption Coefficient of Atmospheric Dust and other Strongly Absorbing Powders," ECOM-5565, July 1975.

2. Avara, Elton, P., "Mesoscale Wind Shears Derived from Thermal Winds," ECOM-5566, July 1975.

3. Gomez, Richard B., and Joseph H. Pierluissi, "Incomplete Gamma Function Approximation for King's Strong-Line Transmittance Model," ECOM-5567, July 1975.

4. Blanco, A.J., and B.F. Engebos, "Ballistic Wind Weighting Functions for Tank Projectiles," ECOM-5568, August 1975.

5. Taylor, Fredrick J., Jack Smith, and Thomas H. Pries, "Crosswind Measurements through Pattern Recognition Techniques," ECOM-5569, July 1975.

6. Walters, D.L., "Crosswind Weighting Functions for Direct-Fire Projectiles," ECOM-5570, August 1975.

7. Duncan, Louis D., "An Improved Algorithm for the Iterated Minimal Information Solution for Remote Sounding of Temperature," ECOM-5571, August 1975.

8. Robbiani, Raymond L., "Tactical Field Demonstration of Mobile Weather Radar Set AN/TPS-41 at Fort Rucker, Alabama," ECOM-5572, August 1975.

9. Miers, B., G. Blackman, D. Langer, and N. Lorimier, "Analysis of SMS/GOES Film Data," ECOM-5573, September 1975.

10. Manquero, Carlos, Louis Duncan, and Rufus Bruce, "An Indication from Satellite Measurements of Atmospheric CO2 Variability," ECOM-5574, September 1975.

11. Petracca, Carmine, and James D. Lindberg, "Installation and Operation of an Atmospheric Particulate Collector," ECOM-5575, September 1975.

12. Avara, Elton P., and George Alexander, "Empirical Investigation of Three Iterative Methods for Inverting the Radiative Transfer Equation," ECOM-5576, October 1975.

13. Alexander, George D., "A Digital Data Acquisition Interface for the SMS Direct Readout Ground Station — Concept and Preliminary Design," ECOM-5577, October 1975.

14. Cantor, Israel, "Enhancement of Point Source Thermal Radiation Under Clouds in a Nonattenuating Medium," ECOM-5578, October 1975.

15. Norton, Colburn, and Glenn Hoidale, "The Diurnal Variation of Mixing Height by Month over White Sands Missile Range, N.M," ECOM-5579, November 1975.

16. Avara, Elton P., "On the Spectrum Analysis of Binary Data," ECOM-5580, November 1975.

17. Taylor, Fredrick J., Thomas H. Pries, and Chao-Huan Huang, "Optimal Wind Velocity Estimation," ECOM-5581, December 1975.

18. Avara, Elton P., "Some Effects of Autocorrelated and Cross-Correlated Noise on the Analysis of Variance," ECOM-5582, December 1975.

19. Gillespie, Patti S., R.L. Armstrong, and Kenneth O. White, "The Spectral Characteristics and Atmospheric CO2 Absorption of the Ho^{+3}:YLF Laser at $2.05\mu m$," ECOM-5583, December 1975.

20. Novlan, David J. "An Empirical Method of Forecasting Thunderstorms for the White Sands Missile Range," ECOM-5584, February 1976.

21. Avara, Elton P., "Randomization Effects in Hypothesis Testing with Autocorrelated Noise," ECOM-5585, February 1976.

22. Watkins, Wendell R., "Improvements in Long Path Absorption Cell Measurement," ECOM-5586, March 1976.

23. Thomas, Joe, George D. Alexander, and Marvin Dubbin, "SATTEL — An Army Dedicated Meteorological Telemetry System," ECOM-5587. March 1976.

24. Kennedy, Bruce W., and Delbert Bynum, "Army User Test Program for the RDT&E-XM-75 Meteorological Rocket," ECOM-5588, April 1976.

25. Barnett, Kenneth M., "A Description of the Artillery Meteorological Comparisons at White Sands Missle Range, October 1974 - December 1974 ('PASS' - Prototype Artillery [Meteorological] Subsystem)," ECOM-5589, April 1976.

26. Miller, Walter B., "Preliminary Analysis of Fall-of-Shot From Project 'PASS'," ECOM-5590, April 1976.

27. Avara, Elton P., "Error Analysis of Minimum Information and Smith's Direct Methods for Inverting the Radiative Transfer Equation," ECOM-5591, April 1976.

28. Yee, Young P., James D. Horn, and George Alexander, "Synoptic Thermal Wind Calculations from Radiosonde Observations Over the Southwestern United States," ECOM-5592, May 1976.

29. Duncan, Louis D., and Mary Ann Seagraves, "Applications of Empirical Corrections to NOAA-4 VTPR Observations," ECOM-5593, May 1976.

30. Miers, Bruce T., and Steve Weaver, "Applications of Meterological Satellite Data to Weather Sensitive Army Operations,"ECOM-5594, May 1976.

31. Sharenow, Moses, "Redesign and Improvement of Balloon ML-566," ECOM-5595, June, 1976.

32. Hansen, Frank V., "The Depth of the Surface Boundary Layer," ECOM-5596, June 1976.

33. Pinnick, R.G., and E.B. Stenmark, "Response Calculations for a Commercial Light-Scattering Aerosol Counter," ECOM-5597, July 1976.

34. Mason, J., and G.B. Hoidale, "Visibility as an Estimator of Infrared Transmittance," ECOM-5598, July 1976.

35. Bruce, Rufus E., Louis D. Duncan, and Joseph H. Pierluissi, "Experimental Study of the Relationship Between Radiosonde Temperatures and Radiometric-Area Temperatures," ECOM-5599, August 1976.

36. Duncan, Louis D., "Stratospheric Wind Shear Computed from Satellite Thermal Sounder Measurements," ECOM-5800, September 1976.

37. Taylor, F., P. Mohan, P. Joseph and T. Pries, "An All Digital Automated Wind Measurement System," ECOM-5801, September 1976.

38. Bruce, Charles, "Development of Spectrophones for CW and Pulsed Radiation Sources," ECOM-5802, September 1976.

39. Duncan, Louis D., and Mary Ann Seagraves,"Another Method for Estimating Clear Column Radiances," ECOM-5803, October 1976.

40. Blanco, Abel J., and Larry E. Taylor, "Artillery Meteorological Analysis of Project Pass," ECOM-5804, October 1976.

41. Miller, Walter, and Bernard Engebos," A Mathematical Structure for Refinement of Sound Ranging Estimates," ECOM-5805, November, 1976.

42. Gillespie, James B., and James D. Lindberg, "A Method to Obtain Diffuse Reflectance Measurements from 1.0 to 3.0 μm Using a Cary 17I Spectrophotometer," ECOM-5806, November 1976.

43. Rubio, Roberto, and Robert O. Olsen,"A Study of the Effects of Temperature Variations on Radio Wave Absorption,"ECOM-5807, November 1976.

44. Ballard, Harold N., "Temperature Measurements in the Stratosphere from Balloon-Borne Instrument Platforms, 1968-1975," ECOM-5808, December 1976.

45. Monahan, H.H., "An Approach to the Short-Range Prediction of Early Morning Radiation Fog," ECOM-5809, January 1977.

46. Engebos, Bernard Francis, "Introduction to Multiple State Multiple Action Decision Theory and Its Relation to Mixing Structures," ECOM-5810, January 1977.

47. Low, Richard D.H.,"Effects of Cloud Particles on Remote Sensing from Space in the 10-Micrometer Infrared Region, " ECOM-5811, January 1977.

48. Bonner, Robert S., and R. Newton, "Application of the AN/GVS-5 Laser Rangefinder to Cloud Base Height Measurements," ECOM-5812, February 1977.

49. Rubio, Roberto, "Lidar Detection of Subvisible Reentry Vehicle Erosive Atmospheric Material," ECOM-5813, March 1977.

50. Low, Richard D.H., and J.D. Horn, "Mesoscale Determination of Cloud-Top Height: Problems and Solutions," ECOM-5814, March 1977.

51. Duncan, Louis D., and Mary Ann Seagraves, "Evaluation of the NOAA-4 VTPR Thermal Winds for Nuclear Fallout Predictions," ECOM-5815, March 1977.

52. Randhawa, Jagir S., M. Izquierdo, Carlos McDonald and Zvi Salpeter, "Stratospheric Ozone Density as Measured by a Chemiluminescent Sensor During the Stratcom VI-A Flight," ECOM-5816, April 1977.

53. Rubio, Roberto, and Mike Izquierdo, "Measurements of Net Atmospheric Irradiance in the 0.7- to 2.8-Micrometer Infrared Region," ECOM-5817, May 1977.

54. Ballard, Harold N., Jose M. Serna, and Frank P. Hudson Consultant for Chemical Kinetics, "Calculation of Selected Atmospheric Composition Parameters for the Mid-Latitude, September Stratosphere," ECOM-5818, May 1977.

55. Mitchell, J.D., R.S. Sagar, and R.O. Olsen, "Positive Ions in the Middle Atmosphere During Sunrise Conditions," ECOM-5819, May 1977.

56. White, Kenneth O., Wendell R. Watkins, Stuart A. Schleusener, and Ronald L. Johnson, "Solid-State Laser Wavelength Identification Using a Reference Absorber," ECOM-5820, June 1977.

57. Watkins, Wendell R., and Richard G. Dixon, "Automation of Long-Path Absorption Cell Measurements," ECOM-5821, June 1977.

58. Taylor, S.E., J.M. Davis, and J.B. Mason, "Analysis of Observed Soil Skin Moisture Effects on Reflectance," ECOM-5822, June 1977.

59. Duncan, Louis D. and Mary Ann Seagraves, "Fallout Predictions Computed from Satellite Derived Winds," ECOM-5823, June 1977.

60. Snider, D.E., D.G. Murcray, F.H. Murcray, and W.J. Williams, "Investigation of High-Altitude Enhanced Infrared Backround Emissions" (U), SECRET, ECOM-5824, June 1977.

61. Dubbin, Marvin H. and Dennis Hall, "Synchronous Meteorlogical Satellite Direct Readout Ground System Digital Video Electronics," ECOM-5825, June 1977.

62. Miller, W., and B. Engebos, "A Preliminary Analysis of Two Sound Ranging Algorithms," ECOM-5826, July 1977.

63. Kennedy, Bruce W., and James K. Luers, "Ballistic Sphere Techniques for Measuring Atomspheric Parameters," ECOM-5827, July 1977.

64. Duncan, Louis D., "Zenith Angle Variation of Satellite Thermal Sounder Measurements," ECOM-5828, August 1977.

65. Hansen, Frank V., "The Critical Richardson Number," ECOM-5829, September 1977.

66. Ballard, Harold N., and Frank P. Hudson (Compilers), "Stratospheric Composition Balloon-Borne Experiment," ECOM-5830, October 1977.

67. Barr, William C., and Arnold C. Peterson, "Wind Measuring Accuracy Test of Meteorological Systems," ECOM-5831, November 1977.

68. Ethridge, G.A. and F.V. Hansen, "Atmospheric Diffusion: Similarity Theory and Empirical Derivations for Use in Boundary Layer Diffusion Problems," ECOM-5832, November 1977.

69. Low, Richard D.H., "The Internal Cloud Radiation Field and a Technique for Determining Cloud Blackness," ECOM-5833, December 1977.

70. Watkins, Wendell R., Kenneth O. White, Charles W. Bruce, Donald L. Walters, and James D. Lindberg, "Measurements Required for Prediction of High Energy Laser Transmission," ECOM-5834, December 1977.

71. Rubio, Robert, "Investigation of Abrupt Decreases in Atmospherically Backscattered Laser Energy," ECOM-5835, December 1977.

72. Monahan, H.H. and R.M. Cionco, "An Interpretative Review of Existing Capabilities for Measuring and Forecasting Selected Weather Variables (Emphasizing Remote Means)," ASL-TR-0001, January 1978.

73. Heaps, Melvin G., "The 1979 Solar Eclipse and Validation of D-Region Models," ASL-TR-0002, March 1978.

74. Jennings, S.G., and J.B. Gillespie, "M.I.E. Theory Sensitivity Studies - The Effects of Aerosol Complex Refractive Index and Size Distribution Variations on Extinction and Absorption Coefficients Part II: Analysis of the Computational Results," ASL-TR-0003, March 1978.

75. White, Kenneth O. et al, "Water Vapor Continuum Absorption in the 3.5μm to 4.0μm Region," ASL-TR-0004, March 1978.

76. Olsen, Robert O., and Bruce W. Kennedy, "ABRES Pretest Atmospheric Measurements," ASL-TR-0005, April 1978.

77. Ballard, Harold N., Jose M. Serna, and Frank P. Hudson, "Calculation of Atmospheric Composition in the High Latitude September Stratosphere," ASL-TR-0006, May 1978.

78. Watkins, Wendell R. et al, "Water Vapor Absorption Coefficients at HF Laser Wavelengths," ASL-TR-0007, May 1978.

79. Hansen, Frank V., "The Growth and Prediction of Nocturnal Inversions," ASL-TR-0008, May 1978.

80. Samuel, Christine, Charles Bruce, and Ralph Brewer, "Spectrophone Analysis of Gas Samples Obtained at Field Site," ASL-TR-0009, June 1978.

81. Pinnick, R.G. et al., "Vertical Structure in Atmospheric Fog and Haze and its Effects on IR Extinction," ASL-TR-0010, July 1978.

82. Low, Richard D.H., Louis D. Duncan, and Richard B. Gomez, "The Microphysical Basis of Fog Optical Characterization," ASL-TR-0011, August 1978.

83. Heaps, Melvin G., "The Effect of a Solar Proton Event on the Minor Neutral Constituents of the Summer Polar Mesosphere," ASL-TR-0012, August 1978.

84. Mason, James B., "Light Attenuation in Falling Snow," ASL-TR-0013, August 1978.

85. Blanco, Abel J., "Long-Range Artillery Sound Ranging: "PASS" Meteorological Application," ASL-TR-0014, September 1978.

86. Heaps, M.G., and F.E. Niles, "Modeling the Ion Chemistry of the D-Region: A case Study Based Upon the 1966 Total Solar Eclipse," ASL-TR-0015, September 1978.

87. Jennings, S.G., and R.G. Pinnick, "Effects of Particulate Complex Refractive Index and Particle Size Distribution Variations on Atmospheric Extinction and Absorption for Visible Through Middle-Infrared Wavelengths," ASL-TR-0016, September 1978.

88. Watkins, Wendell R., Kenneth O. White, Lanny R. Bower, and Brian Z. Sojka, " Pressure Dependence of the Water Vapor Continuum Absorption in the 3.5- to 4.0-Micrometer Region," ASL-TR-0017, September 1978.

89. Miller, W.B., and B.F. Engebos, "Behavior of Four Sound Ranging Techniques in an Idealized Physical Enviroment," ASL-TR-0018, September 1978.

90. Gomez, Richard G., "Effectiveness Studies of the CBU-88/B Bomb, Cluster, Smoke Weapon" (U), CONFIDENTIAL ASL-TR-0019, September 1978.

91. Miller, August, Richard C. Shirkey, and Mary Ann Seagraves, "Calculation of Thermal Emission from Aerosols Using the Doubling Technique," ASL-TR-0020, November, 1978.

92. Lindberg, James D. et al., "Measured Effects of Battlefield Dust and Smoke on Visible, Infrared, and Millimeter Wavelengths Propagation: A Preliminary Report on Dusty Infrared Test-I (DIRT-I)," ASL-TR-0021, January 1979.

93. Kennedy, Bruce W., Arthur Kinghorn, and B.R. Hixon, "Engineering Flight Tests of Range Meteorological Sounding System Radiosonde," ASL-TR-0022, February 1979.

94. Rubio, Roberto, and Don Hoock, "Microwave Effective Earth Radius Factor Variability at Wiesbaden and Balboa," ASL-TR-0023, February 1979.

95. Low, Richard D.H., "A Theoretical Investigation of Cloud/Fog Optical Properties and Their Spectral Correlations," ASL-TR-0024, February 1979.

96. Pinnick, R.G., and H.J. Auvermann, "Response Characteristics of Knollenberg Light-Scattering Aerosol Counters," ASL-TR-0025, February 1979.

97. Heaps, Melvin G., Robert O. Olsen, and Warren W. Berning, "Solar Eclipse 1979, Atmospheric Sciences Laboratory Program Overview," ASL-TR-0026 February 1979.

98. Blanco, Abel J., "Long-Range Artillery Sound Ranging: 'PASS' GR-8 Sound Ranging Data," ASL-TR-0027, March 1979.

99. Kennedy, Bruce W., and Jose M. Serna, "Meteorological Rocket Network System Reliability," ASL-TR-0028, March 1979.

100. Swingle, Donald M., "Effects of Arrival Time Errors in Weighted Range Equation Solutions for Linear Base Sound Ranging," ASL-TR-0029, April 1979.

101. Umstead, Robert K., Ricardo Pena, and Frank V. Hansen, "KWIK: An Algorithm for Calculating Munition Expenditures for Smoke Screening/Obscuration in Tactical Situations," ASL-TR-0030, April 1979.

102. D'Arcy, Edward M., "Accuracy Validation of the Modified Nike Hercules Radar," ASL-TR-0031, May 1979.

103. Rodriguez, Ruben, "Evaluation of the Passive Remote Crosswind Sensor," ASL-TR-0032, May 1979.

104. Barber, T.L., and R. Rodgriquez, "Transit Time Lidar Measurement of Near-Surface Winds in the Atmosphere," ASL-TR-0033, May 1979.

105. Low, Richard D.H., Louis D. Duncan, and Y.Y. Roger R. Hsiao, "Microphysical and Optical Properties of California Coastal Fogs at Fort Ord," ASL-TR-0034, June 1979.

106. Rodriguez, Ruben, and William J. Vechione, "Evaluation of the Saturation Resistant Crosswind Sensor," ASL-TR-0035, July 1979.

107. Ohmstede, William D., "The Dynamics of Material Layers," ASL-TR-0036, July 1979.

108. Pinnick, R.G., S.G. Jennings, Petr Chylek, and H.J. Auvermann "Relationships between IR Extinction, Absorption, and Liquid Water Content of Fogs," ASL-TR-0037, August 1979.

109. Rodriguez, Ruben, and William J. Vechione, "Performance Evaluation of the Optical Crosswind Profiler," ASL-TR-0038, August 1979.

110. Miers, Bruce T., "Precipitation Estimation Using Satellite Data" ASL-TR-0039, September 1979.

111. Dickson, David H., and Charles M. Sonnenschein, "Helicopter Remote Wind Sensor System Description," ASL-TR-0040, September 1979.

112. Heaps, Melvin, G., and Joseph M. Heimerl, "Validation of the Dairchem Code, I: Quiet Midlatitude Conditions," ASL-TR-0041, September 1979.

113. Bonner, Robert S., and William J. Lentz, "The Visioceilometer: A Portable Cloud Height and Visibility Indicator," ASL-TR-0042, October 1979.

114. Cohn, Stephen L., "The Role of Atmospheric Sulfates in Battlefield Obscurations," ASL-TR-0043, October 1979.